Democratic and Popular Republic of Algeria
Ministry of Higher Education and Scientific Research
Abbes Laghrour-Khenchela University
Faculty of Sciences and Technology
Department of Science of Matter

Thesis Presented to obtain the degree of

MASTER

Specialty: Physics of Materials

Synthesis and characterization of Nano composite thin layers (ZnO,CuO,ZnO-CuO) deposited by dip coating

Submitted by: BORDJI Abla

To the Jury composed by:

- **Pr. BENSOUICI Fayçal** Supervisor
- **Dr.BAAOUGUE Khaled** Chairman
- **Pr.DJELLOUL Abdelkader** Examier

Acadymic year 2022-2023

بسم الله الرحمن الرحيم

(وَأَنْزَلَ اللَّهُ عَلَيْكَ الْكِتَابَ وَالْحِكْمَةَ وَعَلَّمَكَ مَا لَمْ تَكُنْ تَعْلَمُ وَكَانَ فَضْلُ اللَّهِ عَلَيْكَ عَظِيمًا)

(Allah has revealed to you the Book and wisdom and has taught you that which you did not know. And ever has the favor of Allah upon you been great)

Acknowledgements

I am writing to express my sincere gratitude and appreciation for the invaluable guidance and support of my supervisor Mr,Bensouici Fayçalthroughout the completion of my master's thesis in Materials Physics. Your expertise and mentorship have been instrumental in shaping my understanding of the subject and enhancing my research skills.

I would also like to extend my appreciation to the entire team at the Laboratory of Structures, Properties, and Intermolecular Interactions (LASPI2A), especially to the laboratory director, Mr. Djelloul Abdelkader, and Ms. Iaiche Sabrina. Your collective efforts and collaborative spirit have created a nurturing environment for research and learning. I would like to acknowledge all my teachers in my university jorney.

Additionally, to acknowledge the invaluable support and guidance I have received from the doctoral student, Ms. Kebaili Selwa.Without forgetting the doctoral student, Ms.Allouche Romaissa.

I would also like to express my gratitude to the Chemistry and Molecular Engineering Laboratory (LCIMN) at the Faculty of Sciences, Farhat Abbas University, Stif 1.

Lastly, I would like to extend my heartfelt thanks to my family. Their unwavering support, encouragement, and understanding have been the pillars of strength throughout my academic pursuits. Their belief in my abilities has fueled my determination to succeed, and for that, I am eternally grateful.

Once again, I would like to express my deepest appreciation to all those mentioned above. Your guidance, support, and encouragement have been invaluable, and I am truly honored to have had the opportunity to learn from such exceptional individuals and institutions.

Bordji Abla

Contents

Contents

Contents

Contents

List of Figures

List of table

Nanomaterials have garnered significant attention due to their unique optical, electrical, and mechanical properties that are not found in bulk materials.

Zinc oxide (ZnO) and copper oxide (CuO) are among the most researched metal oxides, owing to their coexistence of electrical and optical properties, n-type and p-type classification, and wide bandgap of 3eV or more.

These two materials are versatile and are employed in applications such as gas sensors, photodetectors, photocatalysis, and solar cells .In addition we are interesting with the effect of the pn heterojunction CuO-ZnO. Synthesis of metal oxides can be achieved through various methods such as spray pyrolysis, electron beam deposition, and sol-gel dip-coating. The present study utilizes sol-gel dip-coating, as it is a low-temperature and simple deposition method with precise control.

The prepared thin films were characterized using X-ray diffraction, atomic force microscopy,Fourier Transform Infrared, and UV-visible spectrophotometer to determine their structural, morphological, and optical properties.

This study's first chapter provides a background on nanomaterials, Zinc Oxide, Copper Oxide, and thin film deposition techniques, as well as their applications.

The second chapter details the experimental procedure and a bibliographic review of different characterization methods.

The final chapter presents the obtained results and discusses the different properties of the prepared thin layers and multi-thin layers.

A concluding section summarizes the key findings of this thesis.

ChapterI:

Background on: Zinc Oxide and Copper Oxide Nanomaterials ,Thin layers and their applications.

Introduction of the chapter

In this chapter, we aim to provide an overview of key background information and fundamental concepts pertaining to nanomaterials, with a specific focus on ZnO and CuO. These two materials are the primary subjects of investigation in this thesis. We will also delve into the topic of thin films, including their definition, methods of deposition, and properties, specifically those of ZnO and CuO thin films. Additionally, it is imperative that we explore the various application fields in which these thin films find practical use.

I.1.Nanomaterials

I.1.1 Definition

Nanomaterials are a class of materials characterized by having at least one dimension that is less than approximately 100 nanometers in size. At this scale, fundamental properties of materials undergo significant changes, prompting researchers to investigate these changes and report their findings.

The pursuit of enhancing and regulating various properties of materials at the nanoscale has given rise to numerous applications of these materials. These applications include solar cells, photodetectors, electroluminescent diodes, gas sensors, and biosensors....[1]

I.1.2 Classification of nanomaterials

Extensive research has been conducted in the field of nanotechnology, resulting in the discovery of various forms of nanomaterials. As a result, it has become necessary to establish nomenclatures that can classify these materials. Nanomaterials can be classified into four dimensions - 0-D, 1-D, 2-D, and 3-D (bulk cases) - based on their dimensions, as illustrated in Figure I.1. Depending on the degree of confinement, the density of states (DOS) - the number of electronic states per unit of volume and energy - is significantly altered for different types of nanostructures, as demonstrated in Figure I.2 and explained below. [2]:

- **0-dimension**

In the 0-D system, for example the quantum dot, the electrons are confined in their movement in the three directions.

- **1-dimension**

In the 1-D system, such as nanofibres and nanorods, the electrons are free to travel in one direction and confined in the other two directions.

- **2-dimension**

In the 2D system, for example the nanowires, nanoplates, electrons can easily move in two directions and are confined in one direction.

- **3-dimension**

In the 3D system, the bulk case, the electrons are free to move in all three directions and there is no confinements and limitations.

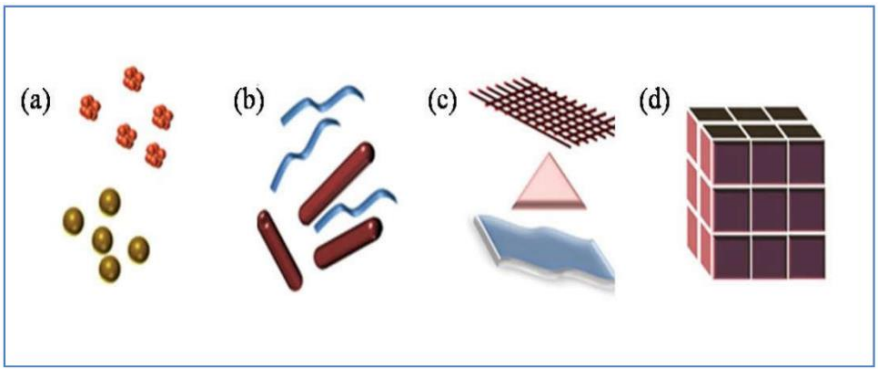

Figure I. 1 Classification of Nanomaterials (a) 0D spheres and clusters,(b) 1D nano-fibers, wires and rods, (c) 2D films, plates and networks, (d) 3D nanomaterials [2].

I.1.3 .Zinc Oxide and its general properties

The II-VI compound semiconductors are of great importance due to their applications in various electro-optic devices. In materials science, Zinc oxide (ZnO) is called II-VI semiconductor because zinc and oxygen belong to the 2nd and 6th groups of the periodic table, respectively. It usually appears as a white powder, nearly insoluble in water. Zinc oxide (ZnO) is a wide bandgap (3.3 eV at room temperature) semiconductor that is desirable for many applications. It is attractive for forming various forms of nanostructures, such as nanorods, nanowires, and nanobelts [3]. Transparent transistors fabricated from ZnO have been reported. With its high exciton binding energy, ZnO is a good candidate for room temperature UV lasers. Its large piezoelectric constant is promising for ultrasonic transducers. ZnO is transparent and electrically conductive, making it an ideal material for solar cell windows. The mineral form of ZnO can be found in nature and is known as Zincite. Zinc oxide has the hexagonal wurtzite structure. ZnO nanomaterials are promising candidates for

nanoelectronic, optoelectronic and solar cells devices [4]. Compared with other semiconductor materials, ZnO has higher exciton binding energy (60 meV), is more resistant to radiation, and is multifunctional with uses in the areas as a piezoelectric, ferroelectric and ferromagnetic [5].

Some important physical properties of ZnO semiconductorrs are given in the table below [6]:

***Table I.1**:Physical properties of ZnO semiconductors*

Property	**Value**
Lattice Parameters	a= b=3.25 Å c=5.21 Å
Stable crystal structure	Wurtzite
Density	5.606 gm/cm^3
Melting point	1975 ^oC
Dielectric constant	8.66
Refractive index	2.008
Energy gap	3.4 eV, direct
Exciton binding energy	60 meV
Effective mass Electron/Hole	0.24 m_o/0.59 m_o
Electron mobility	100-200 cm^2/Vs
Hole mobility	5-50 cm^2/Vs
Bulk young modulus	111.2±4.7 GPa

Crystal structure zinc oxide

Zinc oxide crystallizes in three forms: hexagonal wurtzite, cubic zincblende, and the rarely observed cubic rocksalt. The wurtzite structure is most stable at ambient conditions and thus most common. The zincblende form can be stabilized by growing ZnO on substrates with cubic lattice structure. In both cases, the zinc and oxide centers are tetrahedral. Hexagonal and zincblende polymorphs have no inversion symmetry . This and other lattice symmetry properties result in piezoelectricity of the hexagonal and zincblende ZnO [7].

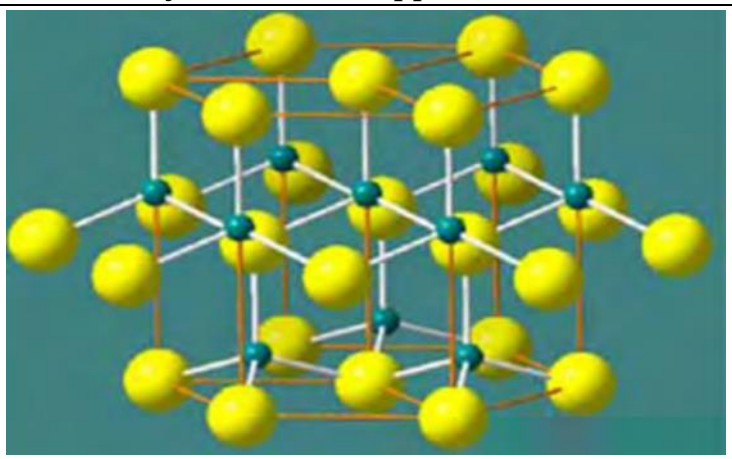

FigI.2: Wurtzite structure of ZnO (lagre ball-Zn, small ball-O)

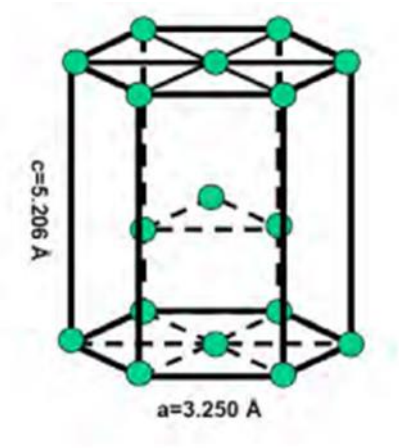

Fig I.3:Hexagonal close packed (hcp) structure of ZnO.

I.1.4. Copper Oxide and its general properties

Copper (II) oxide (CuO) is another metal oxide semiconductor having narrow band gap ~ 1.2 eV in bulk. CuO has monoclinic crystal structure as shown in figure 2.3, and belongs to the space group 2/m. The copper atom is coordinated by four oxygen atom in a square planer configuration [8]. It is intrinsically ptype semiconductor. CuO draw much attention since the starting growth material is inexpensive and easy to get, and the methods to prepare these materials are of low cost .CuO nanostructures have stimulated intensive research due to their high surface area to volume ratio. [8].

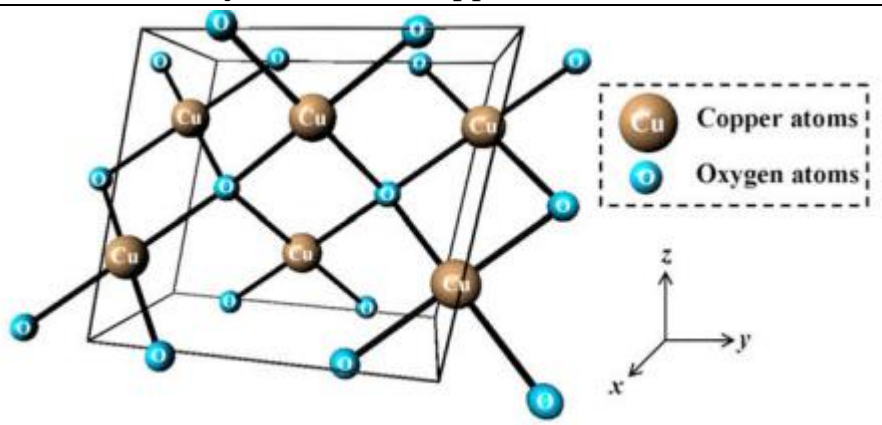

Fig I.4: the monoclinic crystal structure of CuO [9]

Some important physical properties of CuO semiconductors are given in the table below [6]:

TableI.2: Physical properties of CuO semiconductors

Property	Value
Lattice parameters	a=4.68 Å b=3.42 Å c=5.13 Å
Crystal structure	Monoclinic
Density	6.32 g/cm^3
Melting point	1134 ^{o}C
Dielectric constant	18.1
Refractive index	1.4
Energy gap	1.2 eV, direct
Hole mobility	0.1-10 cm^2/Vs

I.2. Thin layers of nanostructures metal oxides

I.2.1. Thin Layer's definition

Any solid or liquid object with one of its dimensions very much less than that of the other two may be called a 'thin film'. Thin film devices would typically be about 5 to 50 µm thick in contrast to bulk devices, which are about 50 to 250 µm thick [9]. If the growth is atom by l atom or molecule by molecule it is called thin film and if the growth is grain by grain it is thick film.The limit between "thin" and "thick" films cannot generally be defined, although

literature sometimes gives an arbitrary value of 1 µm, basically, a film can be considered as "thin" when its properties are significantly different from the bulk. Thin films can be prepared from a nearly infinite range of compositions such as conductive materials, insulators, refractory (oxides, nitrides, carbides) and polymers among others. The structure of the deposited films can be mono or multilayer. Which explain the wide several of their applications: microelectronics, optics, chemistry and mechanics…etc [10].

I.2.2. Thin film deposition methods

The processes for producing thin films are divided into two types, the physical and the chemical methods.

I.2.2.1. Physical vapor deposition (PVD)

Physical Vapor Deposition (PVD) techniques encompass various methods, including evaporation, spraying in all its forms, and laser ablation. Among these methods, the most commonly used PVD techniques are molecular beam epitaxy and cathodic sputtering.

I.2.2.1.1. Sputtering

Sputtering is a deposition technique that is capable of depositing various materials, including metals, refractory materials, dielectrics, and ceramics. The underlying principle of this technique involves bombarding the target material - the material to be deposited - with neutral gas ions, typically argon. The impact of the ion bombardment results in atoms being dislodged from the target material and deposited onto the substrate positioned in front of the target. If the discharge gas is chemically neutral, the sputtering process is referred to as simple sputtering. Conversely, if the discharge gas comprises active gases such as oxygen (O_2) or nitrogen (N_2), the sputtering process is known as reactive sputtering. The basic operational process of sputtering is illustrated in Figure I.5. [11]

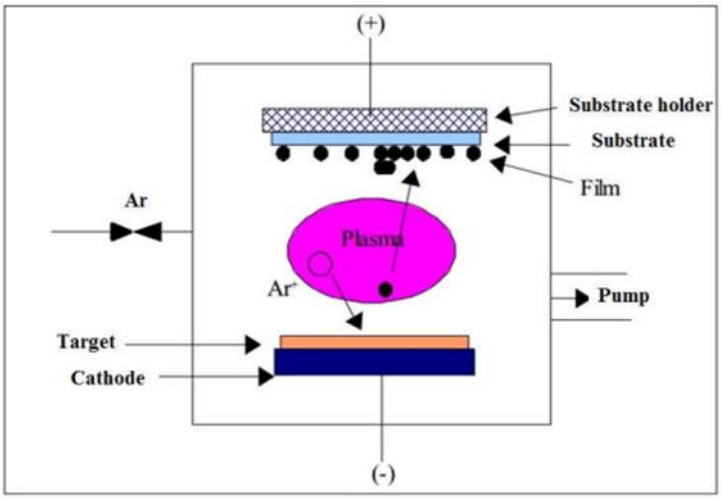

Figure I.5The operating principle of sputtering [11].

There are two types of cathodic sputtering depending on the mode of creation of the plasma or the nature of the target (conductive or insulating): direct cathodic sputtering (DC) only in the case of the sputtering of conductive materials and sputtering radiofrequency (RF) which allows the spraying of conductive materials or insulating materials. There are many parameters that affect the deposition process such as base vacuum, sputter gas pressure during deposition, sputter power, target and substrate temperature, etc…The magnetron device has been used to limit the disadvantages and increase the efficiency of the sputtering[11].

I.2.2.1.2. Molecular Beam Epitaxy (MBE)

The term "epitaxy" is derived from two Greek words - "epi," meaning "on," and "taxi," meaning "arrangement." It refers to the process of creating a monocrystalline layer, known as the epitaxial layer, on a monocrystalline substrate. [12].

Molecular beam epitaxy (MBE) is a technique that enables the growth of high-quality, low-temperature thin films with very low roughness in an ultra-high vacuum environment ($<10^{-10}$ Tor). The underlying principle of this technique is illustrated in Figure I.6 and involves the deposition of atomic or molecular fluxes onto a monocrystalline substrate that has been heated to a specific temperature. [13].

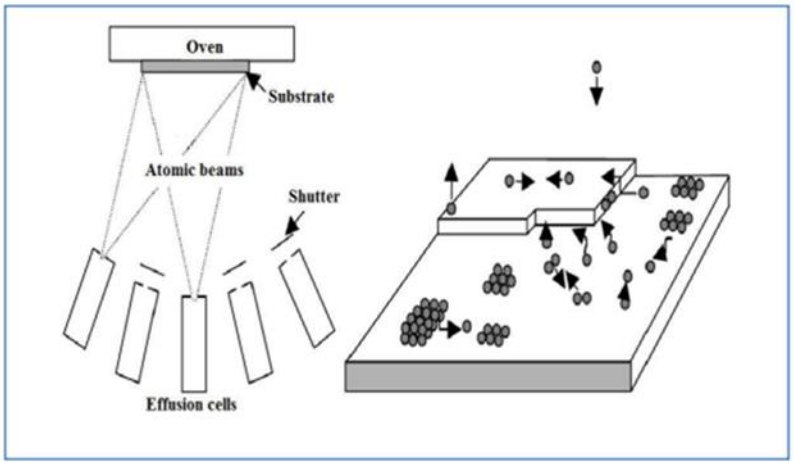

Figure I. 6 the operating principle of MBE [14].

As shown in Figure I.6, the growth process of the molecular beam epitaxy can be summarized in the following steps [14]:

1) Deposition of atoms onto the surface of the substrate

2) Nucleation process (creation of di-atomic islands)

3) Growth of islands by coalescence

4) Formation of a layer by coalescence of islands

I.2.2.1.3. Pulsed Laser Deposition

Pulsed Laser Deposition (PLD) is a deposition technique that offers the benefit of transferring the stoichiometry of the target material to the prepared layer. In this method, a laser beam is focused on a depositing material or target, which is placed inside an ultrahigh vacuum chamber. When the laser beam is directed at the target material, a dense and light vapor or plasma is generated, which causes a portion of the material to be pulled away from the target and deposited onto the substrate that is positioned opposite to the target, as depicted in Figure I.7. [15].

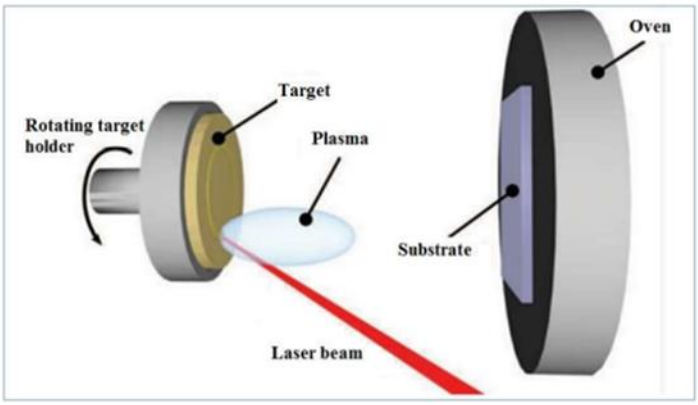

Figure I. 7 Schematic diagram of the Pulsed Laser Deposition (PLD) technique [15].

I.2.2.2. Chemical deposition

I.2.2.2.1. Chemical Vapor Deposition (CVD)

The CVD technique consists of developing materials in the form of thin layers from gaseous precursors that chemically react to form these layers on a heated substrate [16], as shown in figure I.8. The CVD process can be summarized in five steps [17]:

- Transporting reactive gas species (or species) to the substrate.
- Adsorption of the reactants on the surface.
- Surface reaction and film growth.
- Desorption of volatile secondary products.
- Transport and evacuation of gaseous products to the reactor outlet.

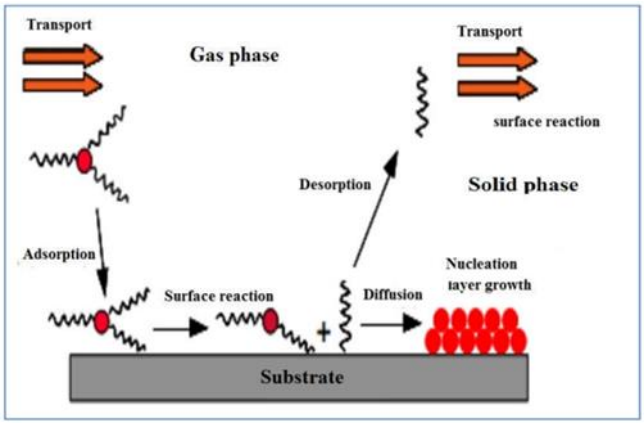

Figure I. 8 The main steps of deposition by the CVD method [12].

I.2.2.2.2. Spray Pyrolysis

The spray pyrolysis is a deposition technique used to prepare thin and thick layers, ceramic coatings and powders. As shown in fig I.9, fine droplets of the precursor solution (containing the material that is to be deposited) are sprayed with a sprayer (nozzle) on a heated substrate. The temperature of the substrate allows the evaporation of the solvents and activates the chemical reactions between the compounds to form the desired layer [18].

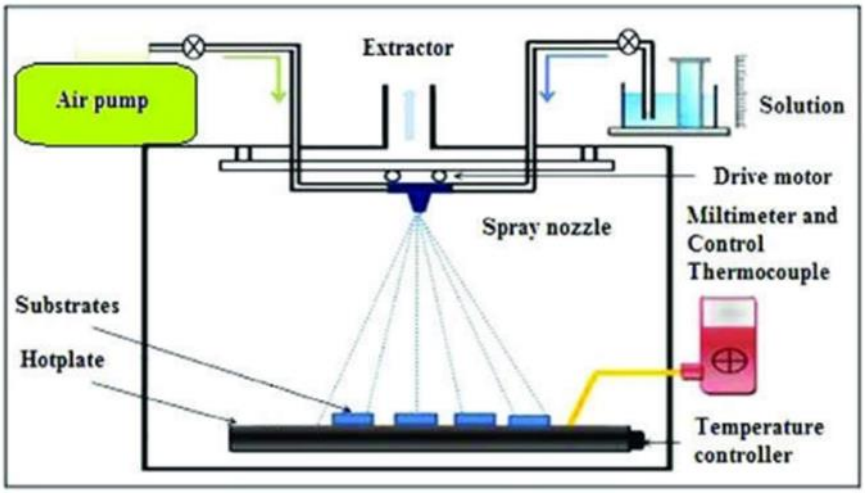

Figure I. 9 Schematic of spray pyrolysis technique [18]

I.2.2.2.3. Sol-Gel

The term sol-gel corresponds to the abbreviation "solution-gelation". The sol-gel method,figure I.10, used to manufacture various materials such as ceramics, powders, fibers, and thin films and is particularly well suited for producing coatings such as thin layers of oxides . Its principle is based on chemical reactions of a chemical precursor consisting of metal atoms of the material that we want to deposit in a solution (solvent) to form an oxide network at an infinite viscosity called "gel", depending on the nature of the precursors used. We distinguish two synthetic voices [19]:

- Inorganic route: obtained from metal salts such as nitrates, sulfates, chlorides, or acetates; dissolved in an aqueous solution.
- Organometallic route: The most frequently used precursor is metal alkoxides in organic solutions.

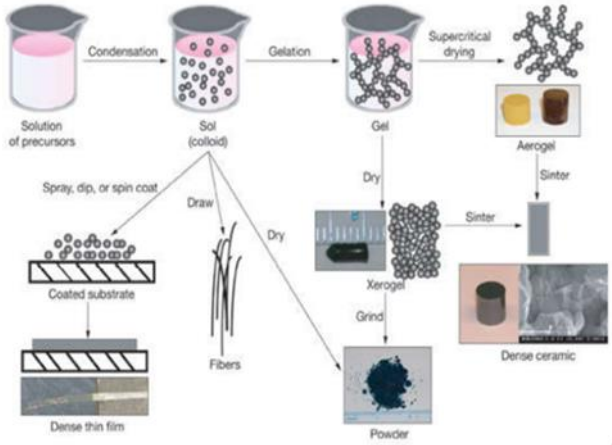

Figure I. 10 Synthesis of various forms of materials by the sol-gel method [19].

I.2.2.2.3.1. Chemical reactions

In the sol-gel method, the chemical mechanism usually decomposes in two stages hydrolysis and condensation. Each obtained gel is linked to chosen appropriate materials.

a. Hydrolysis

It is a reaction between a molecule of water and an alkoxide, allowing the releasing of a molecule of alcohol in three stages illustrated in figure I.11:

- The fixing of a molecule of water on the metal atom M.
- Transfer of proton from the water molecule.
- The departure of an R-OH group carried out by a balanced reaction process.

M-(OR)n+ H2O → OH-M-(OR)n-1 + R-OH

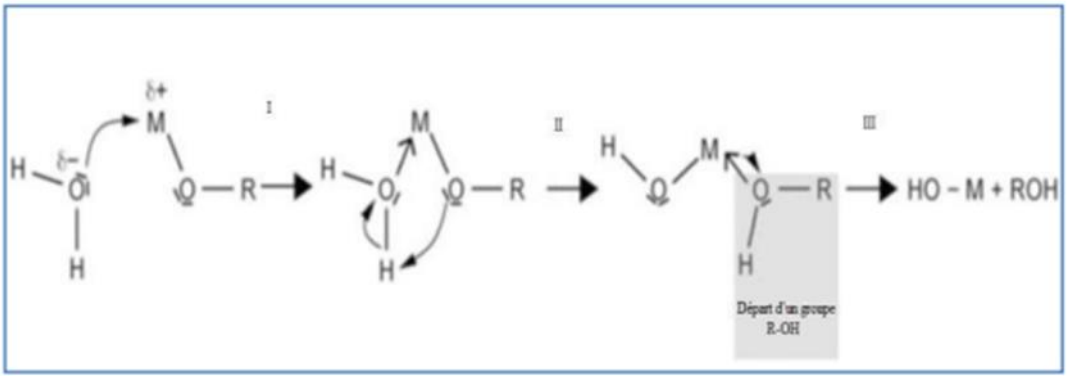

Figure I. 11 Hydrolysis Mechanism of alkoxides M-(OR)n [20].

b. Condensation

The condensation reactions begin after the appearance of the hydroxyl groups and lead to the formation of bonds or metalloxane bridge "M-O-M". The condensation reaction can take place between the different groups. The reaction of the groups (OH-M- (OR) n-1) between them gives a molecule of water (it is the oxolation), the reaction is written:

OH-M-(OR)n-1+ OH-M-(OR)n-1→ (OR)n-1 -M-O-M-(OR)n-1 + H2O

The reaction of the groups (OH-M- (OR) n-1) with remaining non-hydrolyzed groups MOR giving an alcohol molecule R-OH (it is the alkoxolation) follows the reaction:

OH-M-(OR)n-1+ M-(OR)n → (OR)n-1 -M-O-M-(OR)n-1 + R-OH

The condensation reaction mechanism is related to the hydrolysis reaction and therefore the parameters which influence the hydrolysis are also influencing the mechanism and the kinetics of the condensation reaction and consequently the characteristics of the obtained gel [21].

c. The sol-gel transition

The reactions above (hydrolysis and condensation) lead to the formation of a gel consisting of M-O-M chains (or M-OH-M) and polymeric clumps, the size of which increases with time. The sol-gel transition point is achieved when the viscosity becomes infinite [21].

I.2.2.2.3.2. Sol-gel deposition techniques

In the field of research, the thin layers prepared by the sol-gel process are widely known and are used in various applications. The most used techniques are dip-coating and spincoating.

a. Spin-coating

This method consists of centrifuging a solution deposited in excess on a substrate. It has the advantage of being easily implemented and also it gives very good results on flat substrates of small areas (a few cm2) for moderate investments. We can distinguish four main steps in this technique, as shown in figure I.12.

1) The deposition of the solution.

2) At the start of the rotation, the acceleration phase causes the liquid to flow towards the outside of the support.

3) The constant speed rotation allows the ejection of excess liquid in the form of droplets and the reduction of the thickness of the film uniformly.

4) Evaporation of the more volatile solvents which enhances the reduction in the thickness of the deposited film.

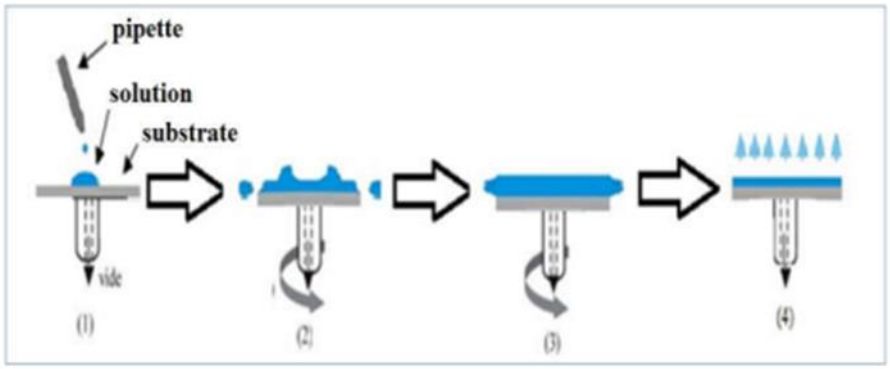

Figure I. 12 The four deposition steps by the spin-coating technique [21].

The properties of the films prepared by this technique depend on the intrinsic parametersof the solution (viscosity, density, etc.) and the deposition parameters (speed and duration ofrotation, acceleration, etc.)

b. Dip-coating

This technique used in this work consists of immersing the substrate in the solution containing the "sol" and removing it under very controlled and stable conditions to obtain a film of a regular thickness (fig I.13). In general, the process can be separated into three important steps:

- Immersion & dwell time: the substrate is dipped in the precursor solution at a constant speed and followed by a certain dwell time to allow sufficient interaction time of the substrate with the solution.
- Deposition: the substrate is pulled upwards at a constant speed (film deposition: Excess liquid will drain from the surface).
- Evaporation: the solvent evaporates by hot drying to form the thin films which can also be treated by annealing at a high temperature to improve their crystallization.

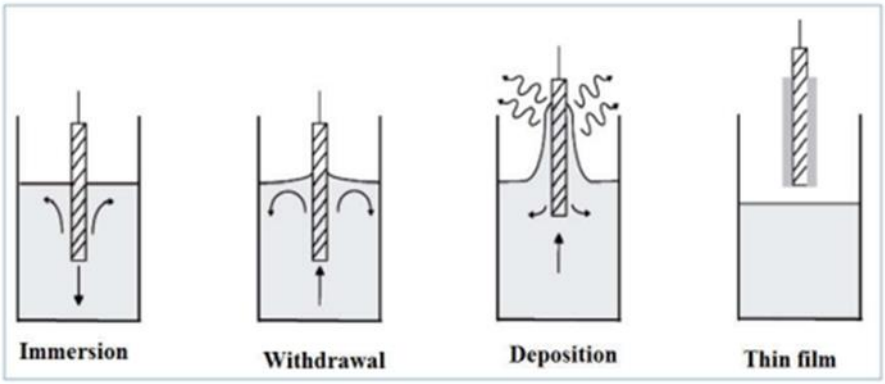

Figure I. 13 The different stages of the dip-coating technique [22].

I.2.2.2.3.3. Advantages and disadvantages of the sol-gel process

a. The sol-gel process has many advantages, including:

- The possibility of deposition of thin layers of oxides at low temperatures
- The possibility of doping (relatively simple during the preparation of the sol)
- The ability of deposition on large substrates
- High purity and homogeneity thin film
- It also allows for multi-component coatings
- Deposition of thin layers on both sides of the substrate (dip-coating).

b. The disadvantages of the sol-gel process:

- The very high cost of some precursors
- Certain chemicals are dangerous to human health.
- Often a long process time.

I.2.3. ZnO and Copper Oxides Thin films and their properties

I.2.3.1. ZnO Thin films

ZnO thin films fabricated for various industrial applications .Several techniques were proposed for the fabrication of ZnO thin films to modify its opticalproperties, including both physical and chemical processes.

Structural and optical properties of ZnO thin films prepared via the sol–gel technique, using a variety of inorganic and organic precursors under different deposition conditions. Post-heat treatment is one of the factors that plays a crucial role in the structural and optical properties of the ZnO thin films through the modification of their crystallinity and surface

roughness. Thermal gravimetric and differential thermal gravimetric analysis (TGA/DTA) of ZnO gelatum by Meng et al. [23] showed that annealing the gel at 500 ◦C ensured complete removal of all the hydroxyl bonds and residues of organic matter. Chaitra et al. [24] investigated the role of annealing temperature (300, 400, and 500 ◦C) on the structural and optical properties of sol–gel-derived ZnO thin films. Thin films annealed at 500 ◦C showed tensile stress and a preferential orientation toward the (002) plane along the c- axis. Raoufi and Raoufi [25], using the same heat treatment conditions, obtained dense ZnO thin films with a (0 0 2) preferred orientation that was enhanced at 500 ◦C. Other authors reported similar observations [26,27].

I.2.3.2. CuO Thin films

Copper oxide thin films could be used for several applications. Several techniques were proposed for the fabrication of CuO thin films including both physical and chemical processes.

CuO thin films prepared via the sol–gel technique, exhibit unique properties that can be tailored by adjusting the deposition parameters. For instance, the thickness of the film can influence its electrical conductivity, as thinner films tend to have higher conductivity due to the reduced scattering of electrons. Similarly, the annealing temperature can alter the crystal structure of the film, leading to changes in its optical and magnetic properties. [28]

I.2.4. Applications of Copper oxide and Zinc Oxide Thin Films

Because of its diverse properties, both chemical and physical, zinc oxide and copper oxide are widely used in many areas. They play an important role in a very wide range of applications. ZnO and CuO exhibit the phenomenon of luminescence (chiefly photoluminescence-emission of light under exposure to electromagnetic radiation). Because of this property they are used in FED (field emission display) equipment, such as televisions. They are superior to the conventional materials, sulfur and phosphorus (compounds exhibiting phosphorescence), because they are more resistant to UV rays, and also have higher electrical conductivity. The photoluminescent properties of both of zinc oxide and copper oxide depend on the size of crystals of the compound, defects in the crystalline structure, and also on temperature [29].

One of the most important applications is in the production of varistors. These are resistors with a non-linear current-voltage characteristic, where current density increases rapidly when

the electrical field reaches a particular defined value. They are used, among other things, as lightning protectors, to protect high-voltage lines, and in electrical equipment providing protection against atmospheric and network voltage surges. These applications require a material of high compactness, since only such a material can guarantee the stability and repeatability of the characteristics of elements made from them2930]. Otherwise, due to their piezoelectric properties, the ZnO and the CuO thin films can be used as pressure sensors.

I.2.4.1. Gas sensor application

The most common sensing materials are metal oxide semiconductors (ZnO and CuO…), which provide sensors with several advantages such as low cost, short response time, wide range of target gases, long lifetime and high sensitivity. As sensors, ZnO and CuO pellets and thin films figure I. 7. The exact fundamental mechanisms that cause a gas response are still controversial, but essentially trapping of electrons at adsorbed molecules and band bending induced by these charged molecules are responsible for a change in conductivity. The negative charge trapped in these oxygen species causes an upward band bending and thus a reduced conductivity compared to the flat band situation. As shown in figure I. 8, when O_2 molecules are adsorbed on the surface of metal oxides, they would extract electrons from the conduction band Ec and trap the electrons at the surface in the form of ions, the oxygen is adsorbed in the form of O^{2-}, O and O^{2-}depending on the operating temperature [30, 31]. This will lead a band bending and an electron-depleted region. The electron-depleted region is so called space-charge layer, of which thickness is the length of band bending region. Reaction of these oxygen species with reducinggases or a competitive adsorption and replacement of the adsorbed oxygen by other molecules decreases and can reverse the band bending, resulting in an increased conductivity. Figure I. 8 schematically shows the structural and band model of conductive mechanism upon exposure to reference gas with or without CO. When gas sensors exposure to the reference gas with CO, CO is oxidized by $O^{-}$and released electrons to the bulk materials. Together with the decrease of the number of surface O^{-}, the thickness of space-charge layer decreases. Then the Schottky barrier between two grains is lowered and it would be easy for electrons to conduct in sensing layers through different grains. However, the mechanism in figure I. 8 is only suitable for n-type semiconducting metal oxides of which depletion regions are smaller than grain size [32].

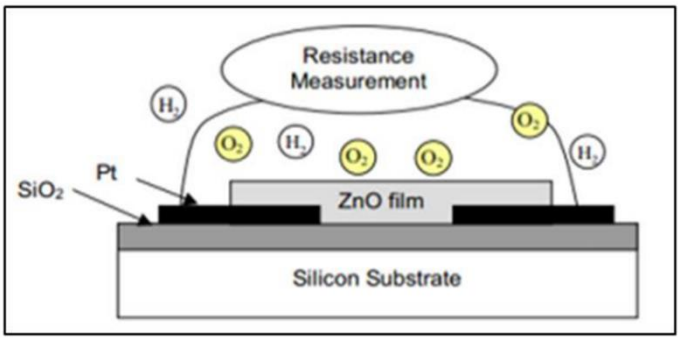

Fig I. 14. ZnO gas sensor structure [32].

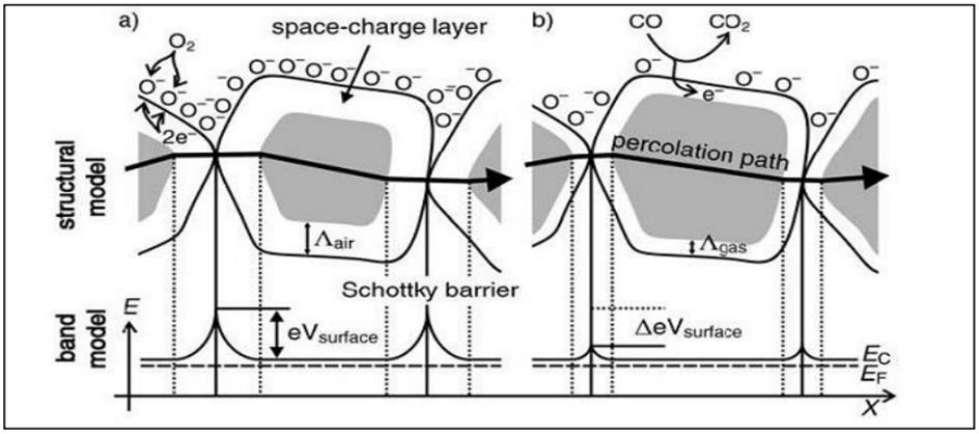

Fig I. 15. Structural and band models of conductive mechanism upon exposure to reference gas (a) With or (b) without CO [31]

I.2.4.2. Photocatalytic activity application

Photocatalysis is defined as the acceleration of a photo reaction in the presence of a catalyst. Since few years, photocatalytic processes involving semiconductor Nanostructures under UV light illumination have been shown to be potentially beneficial and helpful in the treatment of various hazardous pollutants. Different studies have proved this with different pollutants like dyes, drugs, surfactants, pesticides, herbicides, insecticides and fungicides that can be completely mineralized in the presence of ZnO and CuO Nanostructures [29].

I.2.4.3. Transparent electrodes for solar cells application

ZnO is obviously one of the best candidates among semiconductors to produce transparent electrodes for solar cells (thin film solar cells, amorphous silicon solar cells and dye sensitized solar cells (DSSC)) due to its high transparencies and low resistivities, in addition, it can be synthesized easily and inexpensively into different shapes and sizes, and is environment friendly and stable indefinitely [32].

References of the first chapter

[1] Miernicki, M., Hofmann, T., Eisenberger, I. et al. Legal and practical challenges in classifying nanomaterials according to regulatory definitions. Nat. Nanotechnol. 14, 208–216 (2019).

[2] N.ABDELOUAHAB.Preparation and characterization of thin films nanostructures based on ZnO and other oxides,doctorate Thesis,LARBI BEN M'HIDI UNIVERSITY, OUM EL BOUAGHI,

[3] He, J. H., Lao, C. S., Chen, L . J., Davidovic, D. and Wang, Z. L. J., "Large Scale Ni-Doped ZnO Nanowire Arrays and Electrical and Optical Properties" AM. CHEM. SO .Vol. 127, pp 16376-16377, 2005.

[4] Hwang, D. K,, Oh, M. S., Lim, J. H., and ParkJuan, S. J., HaiAn, S., Weii, Z., "ZnO thin films and light-emitting diodes" Phys. D: Appl. Phys. Vol. 40, pp 87–R412, 2007.

[5] Sathananthan, S., Fan, S.W., and Dravid, V.P., "Hydrogen-Sensing Characteristics of Palladium-Doped Zinc-Oxide Nanostructures" Nanoscape Vol. 6, Issue 1, 2009.

[6] S. Zaman,Synthesis of ZnO, CuO and their Composite Nanostructures forOptoelectronics, Sensing and Catalytic Applications, Linköping University Sweden,2012.

[7] Zhou, L., Gu, P., and Zhou, Y., "Piezoelectric f ilm electro-deposition for optical fiber sensor with ZnO coating" Chinese Optics Letters Vol. 6, No. 6, 2008.

[8] Ren, G.; Hu, D.; Cheng, E.W.C.; Vargas-Reus, M.A.; Reip, P.; Allaker, R.P. Characterisation of copper oxide nanoparticles for antimicrobial applications. Int. J. Antimicrob. Agents 2009, 33, 587–590.

[9] A.P. Moura , L.S. Cavalcante , J.C. Sczancoski , D.G. Stroppa , E.C. Paris , A.J.Ramirez ,J.A. Varela , E. Longo Structure and growth mechanism of CuO plates obtainedby microwave-hydrothermal without surfactants,Advanced Powder Technology 21 (2010) 197–202.

[10] M.Dahnoun ."Preparation and characterization of Titanium dioxide and Zinc oxide thin films via Sol-Gel (spin coating) technique for optoelectronic applications"Doctorate Thesis ,University Mohamed Khider of Biskra,2020

[11] Saâd Rahmane, Elaboration et caractérisation de couches minces par spray pyrolyse et pulverisation magnetron, thèse de Doctorat, Universite Mohamed Kheider– Biskra

,2008.

[12] Khachab Hamid, thèse de Doctorat, Modélisation de la croissance épitaxiale par jets moléculaires (MBE) avec la méthode de Monte Carlo Cinétique (KMC), Université Abou-Bekr Belkaid -Tlemcen, 2010.

[13] Gabriel Tourbot, thèse de Doctorat, Croissance par épitaxie par jets moléculaires et détermination des propriétés structurales et optiques de nanofils InGaN/GaN, Université de Grenoble ,2012.

[14] Esteban Martinez-Guerrero, thèse de Doctorat, Elaboration en Epitaxie par Jets Moléculaires des Nitrures d'éléments III en Phase Cubique, Institut National des Sciences Appliquees de Lyon, 2002.

[15] Taabouche Adel, thèse de Doctorat, Etude structurale et optique de films minces ZnO élaboréspar voie physique et/ou chimique, Université Frères Mentouri Constantine I, 2015.

[16] Kefif Kheira, thèse de Doctorat, Elaboration et caractérisation optique des semiconducteurs amorphes et nanocristallins de silicium (a-Si :H, nc-Si :H) et de carbure de silicium (a-SiC :H, nc-SiC :H), Université d'Oran 1, 2015

[17] Maria Magdalena Şovar, thèse de Doctorat, du tri-isopropoxyde auxoxydes d'aluminium par dépôt chimique en phase vapeur : procédé, composition et propriétés des revêtements obtenus, INP Toulouse et Université Polytechnique de Bucarest, 2006.

[18] A. Mennad, "Les techniques de dépôt de couches minces et leurs applications," Revue des Energies Renouvelables, vol. 18, pp. 713–719, 2015.

[19] Ammar Mosbah, thèse de Doctorat, Elaboration et caractérisation de couches minces d'oxyde de zinc, Université Mentouri Constantine , 2009

[20] Lilia Baghriche , thèse de Doctorat, Elaboration et caracterisation des couches mincesd'oxyde de zinc et sulfure de zinc preparees par sprayultrasonique , Universite Freres Mentouri , 2015.

[21] J. Livage, Sol-gel synthesis of solids, Encyclopaedia of Inorganic Chemistry, R. Bruce King and. John Wiley edition, NewYork, 3836-3851, 1994.

[22] F. Collignon, Techniques de l'ingenieur : Cahier technologique Sol-Gel, certech asbl, B-7180 Seneffe – Belgium, 2008.

[23] Meng, X.; Zhao, C.; Xu, B.; Wang, P.; Liu, J. Effects of the annealing temperature on the structure and up-conversion photoluminescence of ZnO film. J. Mater. Sci.

Technol. 2018, 34, 2392–2397.

[24] Chaitra, U.; Kekuda, D.; Rao, K.M. Effect of annealing temperature on the evolution of structural,microstructural, and optical properties of spin coated ZnO thin films. Ceram. Int. 2017, 43, 7115–7122.

[25] Raoufi, D.; Raoufi, T. The effect of heat treatment on the physical properties of sol–gel derived ZnO thin films. Appl. Surf. Sci. 2009, 255, 5812–5817.

[26] O'Brien, S.; Nolan, M.G.; Çopuroglu, M.; Hamilton, J.A.; Povey, I.; Pereira, L.; Martins, R.; Fortunato, E.;Pemble, M. Zinc oxide thin films: Characterization and potential applications. Thin Solid Films 2010,518, 4515–4519.

[27] Arif, M.; Sanger, A.; Vilarinho, P.M.; Cho, M.H. Effect of annealing temperature on structural and opticalproperties of sol–gel-derived ZnO thin films. J. Electron. Mater. 2018, 47, 3678–3684.

[28] M. Dahrula,, Husin Alatasb, Irzamanb,Preparation and optical properties study of CuO thin film as applied solar cell on LAPAN-IPB Satellite,The 2nd International Symposium on LAPAN-IPB Satellite for Food Security and Environmental Monitoring 2015, LISAT-FSEM 2015

[29] A. Kołodziejczak-Radzimska and T. Jesionowski, "Zinc Oxide-From Synthesis to Application: A Review", Materials, 7(4), (2014), 2833-2881.

[30] C. M. Ghimbeu., J. Schoonman., M. Lumbreras and M. Siadat, "Electrostatic spray deposited zinc oxide films for gas sensor applications", Applied Surface Science, 253(18), (2007) 7483-7489.

[31] C. Wang., L. Yin, L. Zhang, D. Xiang and R. Gao, "Metal oxide gas sensors: sensitivity and influencing factors", Sensors, 10(3), (2010) 2088-2106.

[32] A. B. F, Martinson., J. E. McGarrah., M. O. Parpia, and J. T. Hupp.3"Dynamics of charge transport and recombination in ZnO nanorod array 4ye-sensitized solar cells", Physical Chemistry Chemical Physics, 8(40), 52006) 4655-4659.

Chapter II:

Thin films deposition techniques and characterization tools

Introduction of the chapter

In this chapter, we will discuss the experimental procedure for sol-gel dip coating, starting from the selection and cleaning of the substrate to the preparation of the sol and the dip coating process. We will also explore the different parameters that can affect the film quality, such as sol viscosity, substrate temperature, and withdrawal speed. Moreover, we will cover the various methods of characterization used to analyze the properties of the deposited films, including surface morphology, composition, and crystallinity. Some of the common characterization techniques that we will discuss include scanning electron microscopy (SEM), X-ray diffraction (XRD), Fourier transform infrared (FTIR) spectroscopy, .

Overall, this chapter will provide a comprehensive overview of the experimental procedure for sol-gel dip coating and the various methods of characterization used to evaluate the quality and properties of the deposited films.

II.1. Experimental procedure:

II.1.1. Substrates selection:

We deposited the thin films on glass substrates because of their transparency in the UV-visible range, which is fascinating from an economic point of view but also makes it feasible to obtain excellent optical characterization of thin films.

II.1.2. Substrates cleaning:

This step is very important for obtaining thin films of good quality because the slightest impurity can cause contamination and detachment of the deposited layers. The glass substrates were cleaned with steel ultrasonic cleaner (BAKU-3050) at different stages, as follows:

- Rinse for 10 min in an ultrasonically activated acetone bath.
- Rinse with distilled water.
- Immersion in an ultrasonically activated methanol bath for 5 minutes.
- Rinse with distilled water.
- Immersion in an ultrasonically activated , ethanol bath for 5 minutes.

II.1.3. Solution preparation

For preparing 0,4 M of zinc oxide and 0,4M of copper oxide we using Zinc acetate dihydrate (Zn $(CH_3COO)_2$; $2H_2O$) and copper acetate dihydrate $Cu_2(OAc)_4(H_2O)_2$ as precursor, isopropanol as a solvent and dia_ethanolamine (DEA) ($NH_2CH_2CH_2eOH$) as stabilizer.

II.1.4.Thin films deposition

Thin films of ZnO and CuO, as well as multi-thin films of ZnO/CuO, were synthesized using a dip-coating method and Holmarc's Dip Coating Unit Model No: HO6TH602B, as shown in Figure II.1.

figure II.1:Holmarc's Dip Coating Unit Model

a.CuO Thin filmspreparation

Firstly, the (38 ×25 mm) glass plates (SAIL BRAND, CAT. NO. 7101 China) were cleaned and then dipped into the CuO coating precursor solution at a withdrawal speed of 4*mm/s* using a dip-coating method. The process was conducted at room temperature. After each layer was coated, the film was dried on a hotplate at 300°C for 5 minutes to remove any solvent residue. This deposition process was repeated to create series with 8cycles of thin films on each substrate. Figure 2 shows the results of the deposition.

Figure II.2:CuO Thin films

b.. ZnO Thin filmspreparation

We followed the same procedure and conditions as previously mentioned, but this time we used a ZnO precursor solution that we had prepared.

c. ZnO/CuO multi-thin films preparation

After each deposition of a thin film and its subsequent drying, another thin film was deposited on top of the first in an alternating fashion. We began by depositing a ZnO thin films, followed by a CuO thin films, and so on.

d. 2ZnO/2CuO multi-thin films preparation

In this case we deposited 2 thin layers of the same metal oxide as bottom layers and the two others as top layers .

II.1.5. Annealingprocess

Once the thin films have been dried to remove any solvent residue using conventional thermal methods, the next step is annealing, which is a crucial process in thin film preparation. This step involves using the Nabertherm oven, as shown in Figure II.3, and it facilitates better crystallization, allowing for a transition from amorphous to polycrystalline structures. Additionally, it helps to eliminate any organic residues left over from the precursors used in the solution.

The substrates were placed in the oven, and the temperature was gradually raised in increments of 10°C every 1 minute until it reached 500°C. The oven was then turned off after an hour, and the substrates were allowed to dry, as shown in FigureII.4.

Figure II.3: Nabertherm oven

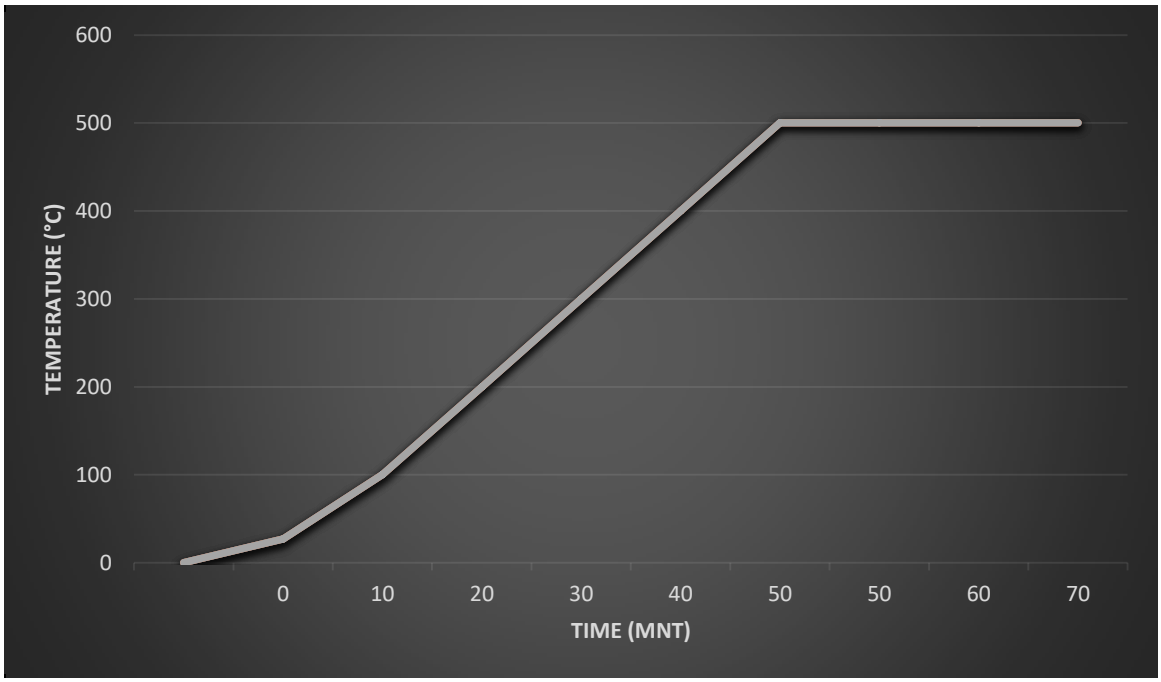

Figure II.4: Evolution of oven temperature

The results of this process are shown in Figure II.5 , II.6,II.7 , II.8.

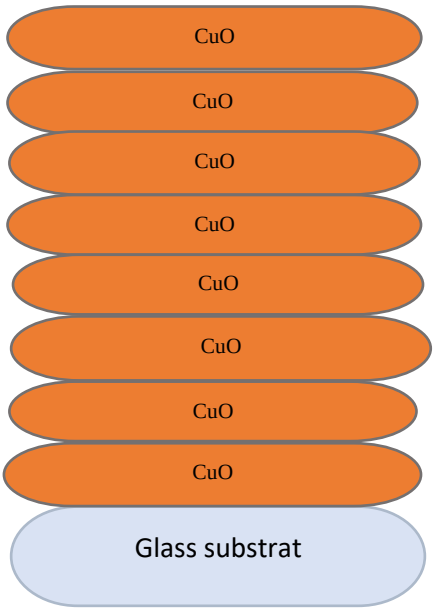

FigureII.5: CuO Thin films

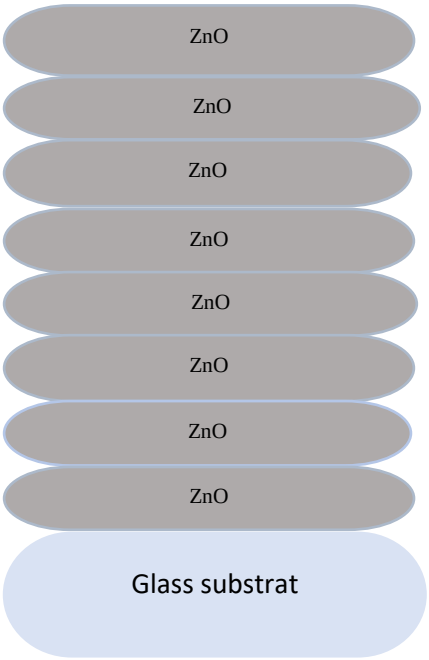

Figure II.6:ZnO Thin films

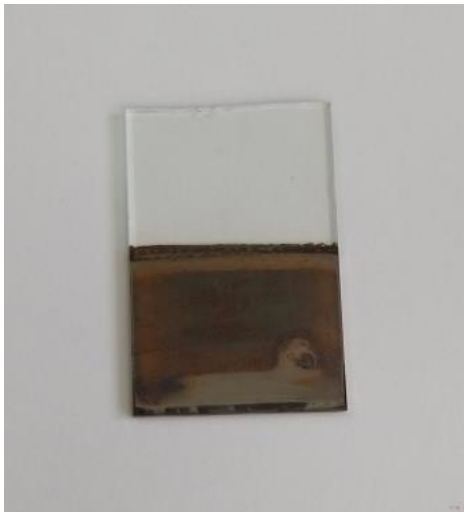

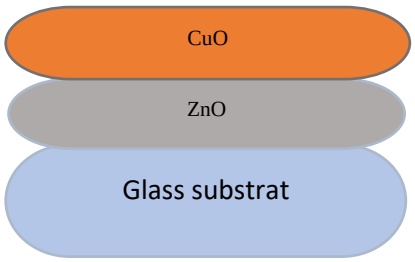

(a)

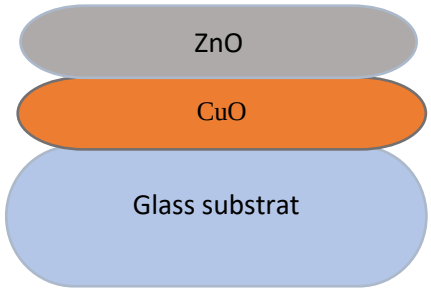

(b)

Figure II.7 : (a) ZnO/CuO multi thin layers,(b :CuO/ZnO multi thin layers

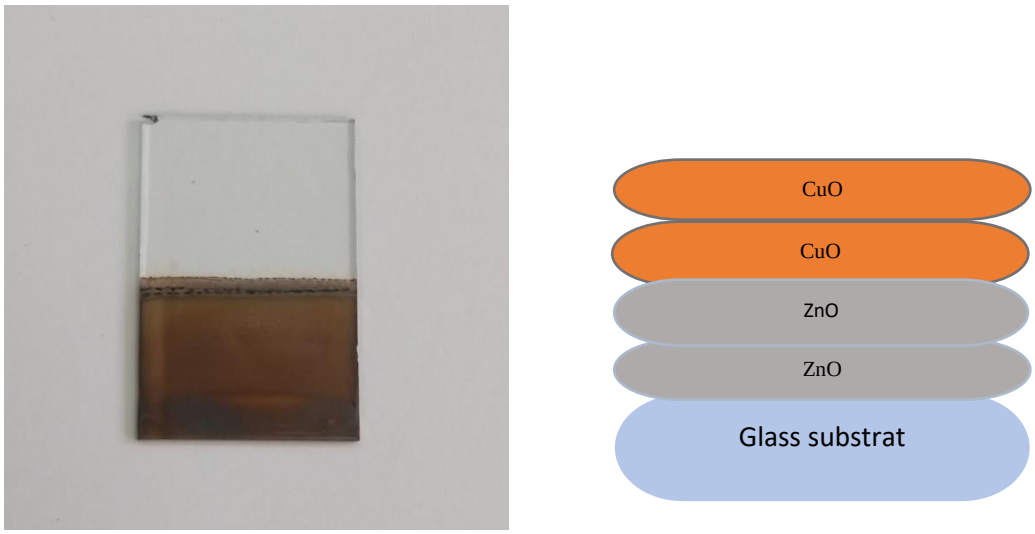

(a)

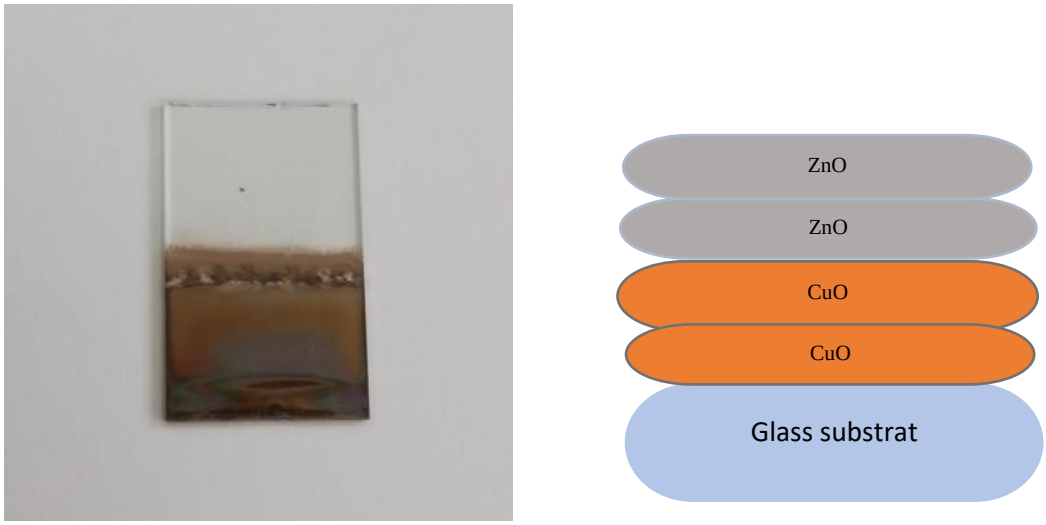

(b)

Figure II.8 : (a) 2ZnO/2CuO multi thin layers,(b :2CuO/2ZnO multi thin layers

II.2. Characterization techniques

II.2.1. Structural characterization using X-Ray Diffraction (XRD)

X-RAY s a structural analysis technique that provides non-destructive means of determining the crystal structure of various materials ,including bulk materials ,powders and thin films. This technique is based on the Bragg law ,which establishes a relation between a diffraction angle θ, the wavelength λ of X-rays, and the distance dhkl between crystallographic planes [1],as shown in FigureII.7.

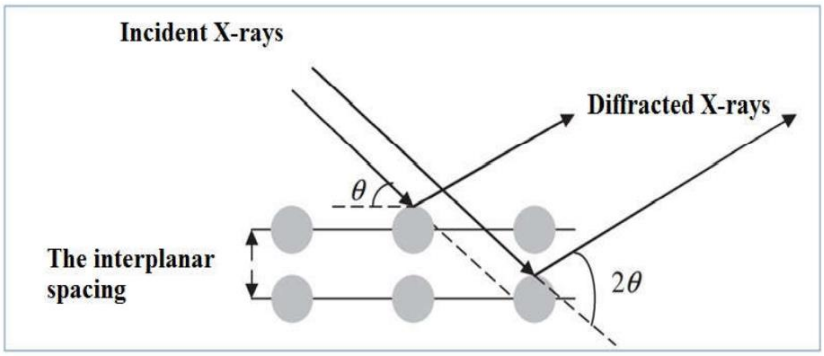

Figure II.9 The Principle of Bragg Law [1].

To perform this technique, an X-ray beam is directed at the sample to be analyzed at a specific angle θ. The intensity of the X-ray beam diffracted by the sample is then recorded as a function of the 2θ angle it forms with the incident X-ray beam, as illustrated in Figure 8. This technique allows for the identification of compounds and/or phases by comparing the obtained results with the reference values listed in the standard files JCPDS (Joint Committee for Powder Diffraction Standards)[2].

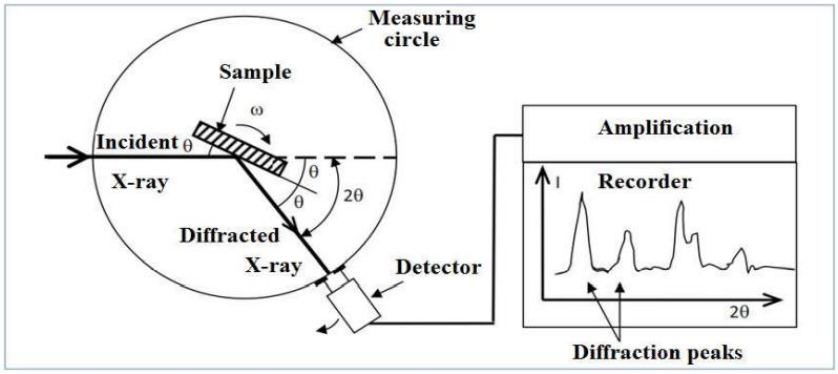

Figure II.10 Schematic diagram of an X-ray diffractometer [2].

By utilizing the spectrum of X-ray diffractions, it becomes feasible to identify various traits of a material that has been crystallized. This includes the orientation of the crystallites, the crystalline phases (indicated by peak position), the level of strain present, and the size of

the crystallites (represented by D). The Scherrer formula [3] can be used to calculate the size of the crystallites by analyzing the width at half height, also known as the FWHM (Full Width at Half Maximum).

$$D = 0.9\ \lambda/\beta\ cos\ \theta \qquad (1)$$

Where:

D: is the average crystallite size in nm.

β: is the width at half height (in radian).

θ: is the diffraction angle (in degrees).

The dislocation density

The dislocation density defined as the length of dislocation lines per unit volume.

It was calculated by the relation [3].

$\delta = 1/D^2$ (2)

Where D is the grain size.

The micro strain

Micro strain refers to a small amount of strain or deformation that occurs within a material or crystal structure. It is defined as the fractional change in length or volume of a material due to a small amount of elastic deformation. It is commonly used to describe the amount of strain or deformation that occurs within a material due to external forces or changes in temperature.

The micro strain of the thin films is estimated using the equation [3]

$\varepsilon = \beta cos\theta/4$ (3)

In this work we used PHILIPS X'PERT diffractometer, FigureII. 11.

FigureII.11 :PHILIPS X'PERTdiffractometer.

II.2.3. Characterization by Atomic Force Microscopy (AFM):

The atomic force microscopy (AFM) is a method that enables the examination of both the topography and physical characteristics of samples at the nanoscale. This technique originated in the 1980s and consists of a flexible lever (cantilever) with a fine tip at the end. The tip scans the surface of the sample by using a piezoelectric ceramic, a laser diode, and a detector that measures the cantilever deflection caused by atomic force during scanning. Through AFM, it is possible to acquire images of surface morphology and roughness, as well as determine the grain size of the samples being analyzed. Figure shows the components of an AFM setup[6].

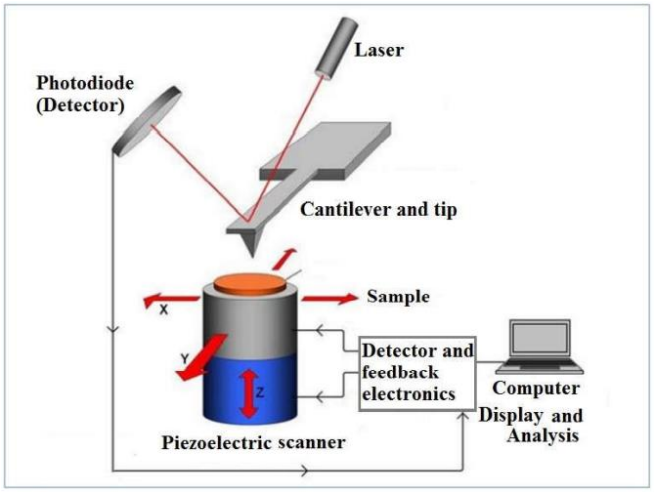

Figure II.12 Schematic explaining the principle of an atomic force microscope [6].

In this work we used HERZAN TS-ISOan Chemistry Ingeniering molecular and Nanostructure Laboratory(LCIMN) ,Faculty of Science ,Ferhat Abbas Setif 1 university .Figure II.14.

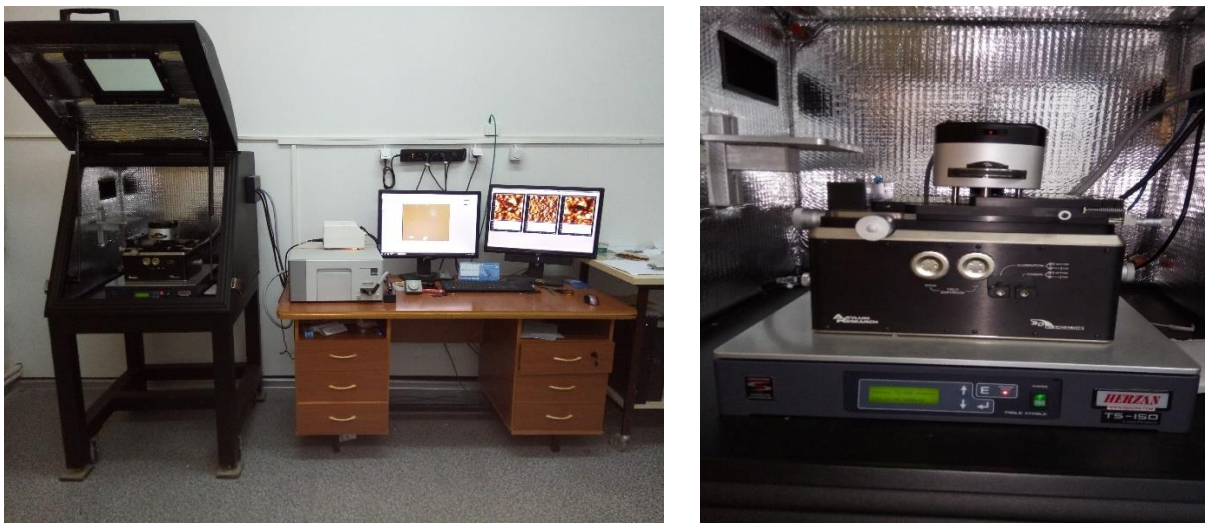

Figure II.13:HERZAN TS-ISOatomic force microscope.

II.2.4. Fourier Transform Infrared (FTIR)

FTIR is a cost-effective method that offers insights into the chemical bonding within a material, especially for non-destructive analysis of solids and thin films. It employs a broad band source of IR radiation that is reflected from the sample, or transmitted in the case of thin samples. The technique identifies the wavelengths at which absorption takes place by measuring the alteration in the intensity of the light as a function of the wavelength. The absorption wavelengths are a result of the vibrations of chemical bonds, which are unique to the type of bond and group of atoms involved in the vibration[7].

Figure II.14:Spectrometer PerkinElmer.

II.2.5. UV-Visible spectrophotometry

UV-Visible spectrophotometry relies on the interaction between matter and electromagnetic radiation within the Ultraviolet-Visible and Infrared spectral domains. By utilizing this technique, we can acquire various optical properties of samples such as transmittance or absorbance curves across UV-visible spectrum wavelengths, determination of band gap energy (Eg), optical absorption threshold, absorption coefficient, refractive index, extinction coefficient, and other related properties[8].operating principle is shown in FigureII.16.

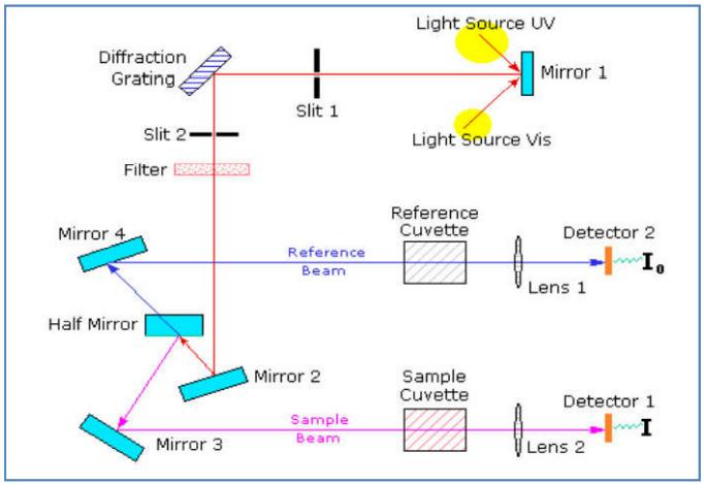

Figure II.15:Schematic representation of the UV-Visible spectrophotometer[8].

The optical gap (Eg) is determined by using the equation [8]:

$$(\propto hv) = A(hv - Eg)^n \qquad (4)$$

A is a constant, α is the absorption coefficient, *hv* the energy of a photon and n is a number depends on the nature of optical transition, can obtain the values 1/2, 2, 3 and 3/2 for direct allowed, indirect allowed, direct forbidden and indirect forbidden transitions, respectively. From the plot of $(\propto hv)^2$versus *hv*, we can estimate the value of optical band gap by extrapolating the linear region to meet *hv* axis.

If we have a spectrum of transmittance and the thickness d of a thin layer we can determine the absorption coefficient by using the Bouguer-Lambert-Beer formula [9]:

$$T = e^{-ad} \qquad (5)$$

In the case where the transmittance T is expressed in (%), the absorption coefficient is given by:

$$\alpha = \frac{1}{d} ln\left(\frac{100}{T\%}\right) \qquad (6)$$

In this work, the experimental measurements are carried out using a Visible UV spectrophotometer of the type CMK.40.7997 which shows on the figure II.17.

Figure II.16: UV-Visible spectrophotometer (CMK.40.7997).

References of the chapter

[1] Liu YANG, Caractérisation de couches minces de ZnO élaborées par la pulvérisation cathodique en continu ,, thèse de Doctorat, Université du Littoral côte d'Opale , 2012.

[2] Tayeb Brouri, , Élaboration et étude des propriétés électriques de couches minces et de nanofils de ZnO, thèse de Doctorat, Université Paris-Est , 2011.

[3] A. Hamrouni, N. Moussa, F. Parrino, A. Di, A. Houas, and L. Palmisano, "Sol – gel synthesis and photocatalytic activity of ZnO – SnO2 nanocomposites," Journal of Molecular Catalysis A: Chemical, vol. 390, pp. 133–141, 2014.

[4] B. Martínez, F. Sandiumenge, L. Balcells, J. Arbiol, F. Sibieude, and C. Monty, "Structure and magnetic properties of Co-doped ZnO nanoparticles," Phys. Rev. B - Condens. Matter Mater. Phys., vol. 72, no. 16, pp. 1–8, 2005, doi: 10.1103 / PhysRevB.72.165202.

[5] P. A. J. Sasanka Deka, "Synthesis and magnetic properties of Mn doped ZnO nanowires," Solid State Commun., vol. 142, no. 4, pp. 190–194, 2007, doi: 10.1016 /j.ssc.2007.02.017.

[6] Younes Mouchaal, thèse de Doctorat, Elaboration et étude de nouvelles électrodes transparentes substituts de l'ITO dans les dispositifs optoélectroniques, Université d'Oran 1 Ahmed Ben Bella, 2016.

[7] L. Herissi, L. Hadjeris, M. S. Aida, and J. Bougdira, "Properties of (NiO)1- x (ZnO) x thin films deposited by spray pyrolysis," Thin Solid Films , vol. 605, pp. 116–120, 2016.

[8] M. Dahnoun; Preparation and characterization of Titanium dioxide and Zinc oxide thin films via Sol-Gel (spin coating) technique for optoelectronic applications, Doctorate Thesis, University Mohamed Khider of Biskra,June 2020.

[9] A. A. Al-Ghamdi, M. S. Abdel-Wahab, A. A. Farghali, and P. M. Z. Hasan, "Structural, optical and photo-catalytic activity of nanocrystalline NiO thin films," Mater. Res. Bull, vol. 75, pp. 71–77, 2016.

Chapter III

Results and discussion

Introduction of the chapter

In this chapter, we present the comprehensive results and characterization of our study, aimed at gaining deeper insights into the properties and behavior of the ZnO and CuO thin layers as well as their multi-thin layers. Through a combination of various analytical techniques, including X-ray Diffraction (DRX), Atomic Force Microscopy (AFM), Fourier Transform Infrared Spectroscopy (FTIR), and UV-Visible Spectroscopy, we elucidate the structural, morphological, chemical, and optical aspects of the material. The findings presented in this chapter shed light on the fundamental characteristics and potential applications of these thin layers, providing a foundation for further exploration and utilization.

III.1. Structural characterization by XRD

X-ray diffraction (XRD) patterns of ZnO thin films deposited on glass substrate ,wich were taken using CuKα (λ = 1.540598Å) source are shown in Figure III.1 .

Matching of observed and standard ‘d’ values of ZnO using X’PERT HIGHHT SCORE PLUS , card No00-036-1451confirms that deposited films fit well with hexagonal wurtzite structure. XRD patterns exhibit strong peaks (100), (002), (101), (102), (110), (103) and (200) on 2θ =32.109 ; 34.788 ; 36.701 ; 46.672 56.984 ; 63.235 ; 68.338 respectively.

The matching is shown in figure III.2.

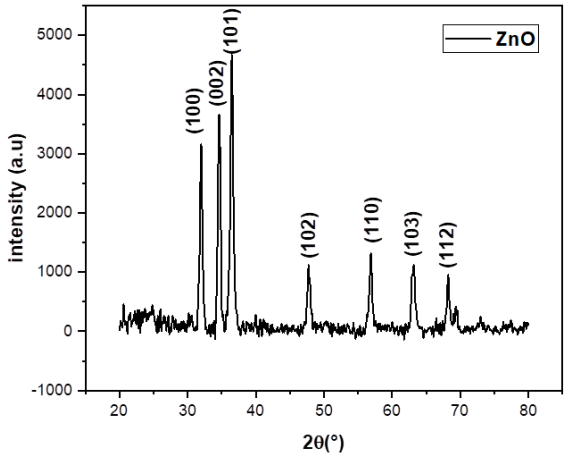

Figure III.1:X ray patterns of ZnO thin films

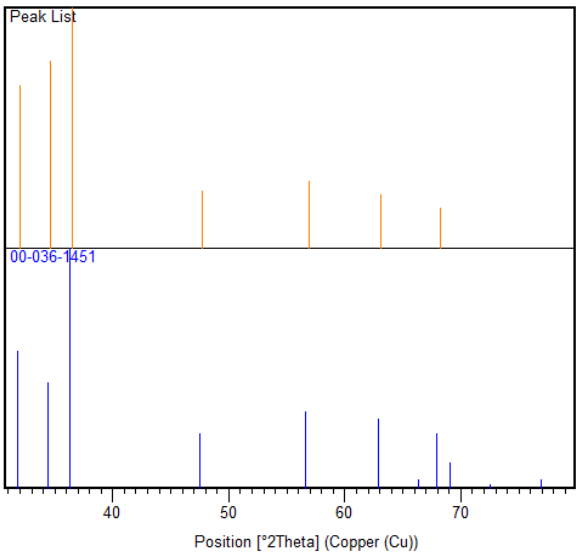

Figure III.2:A Comparison of X-Ray Patterns in Samples and High Score Data Files

X-ray diffraction (XRD) patterns of CuO thin films deposited on glass substrate ,wich were taken using CuKα (λ = 1.540598 Å) source are shown in Figure III.3.

Matching of observed and standard 'd' values of CuO using X'PERT HIGHHT SCORE PLUS , card No 00-041-0254 confirms that deposited films fit well with Monoclinic structure . XRD patterns exhibit strong peaks (1 1 0) ,(-1 1 1) ,(1 1 1) ,(-2 0 2),(0 2 0) on 2θ= 32 .737 ; 35.808 ; 38.975 ; 49.051 ; 53.850 respectively.

The matching is shown in figure III.4.

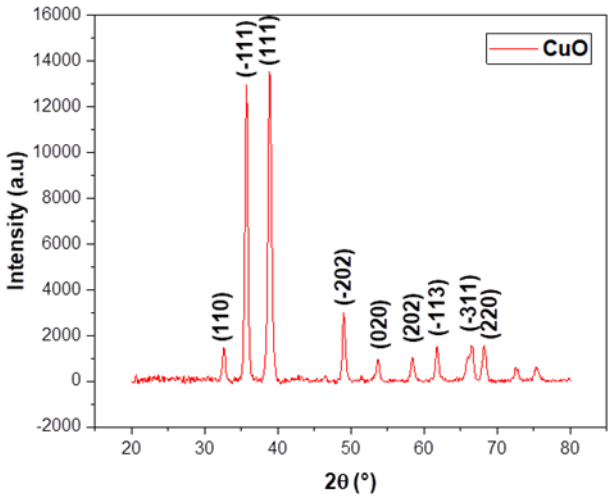

Figure III.3: X ray patterns of CuO thin films

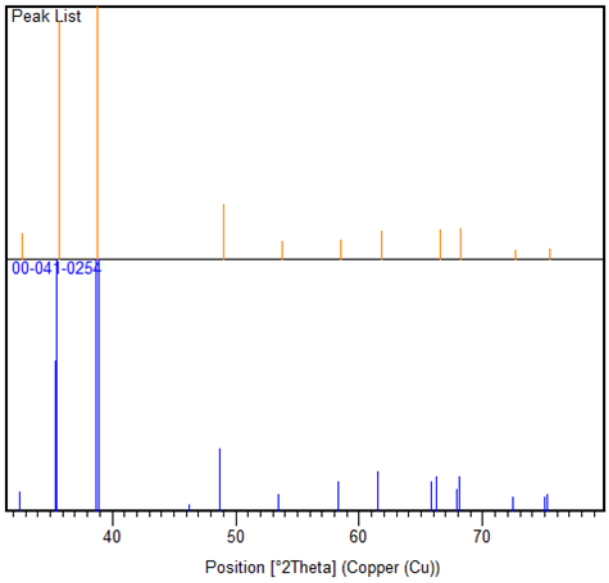

Figure III.4: A Comparison of X-Ray Patterns in Samples and High Score Data Files

X-ray diffraction (XRD) patterns of ZnO/CuO as well as CuO/ZnO thin films deposited on glass substrate ,wich were taken using CuKα (λ = 1.540598 Å) source are shown in FigureIII.5.

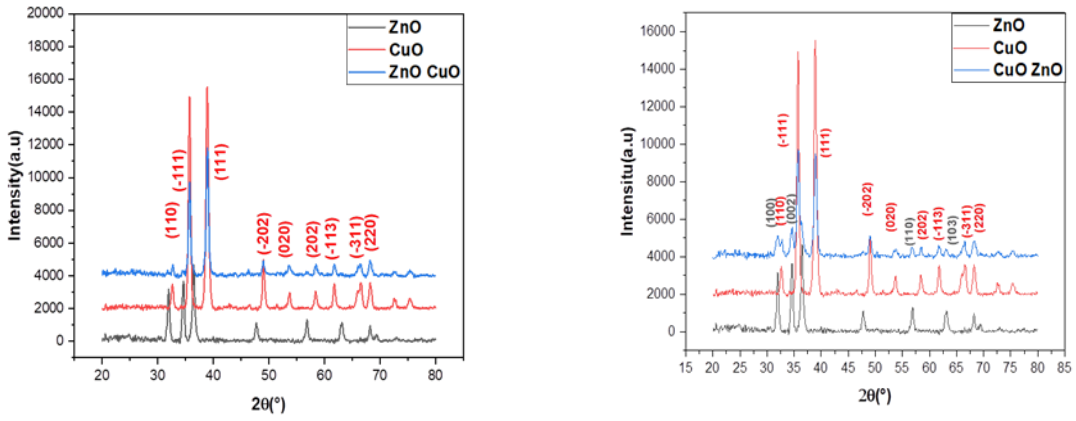

(a) (b)

Figure III.5: X-ray diffraction (XRD) patterns of(a): ZnO/CuO ,(b):CuO/ZnO thin films

We observe that in the case of depositing a thin film of CuO on a thin film of ZnO, only peaks corresponding to CuO are present. However, in the case of depositing ZnO on CuO, some peaks of CuO are observed as follows: (100),(002),(110),(103). Maydue to the larger thickness of CuO compared to ZnO.

The same observation was made in the case of 2ZnO/2CuO and 2CuO/2ZnO multi thin layers as in the case of ZnO/CuO and CuO/ZnO multi thin layers, leading to the conclusion that the thickness does not have an effect on the resulting structure in these cases**.**

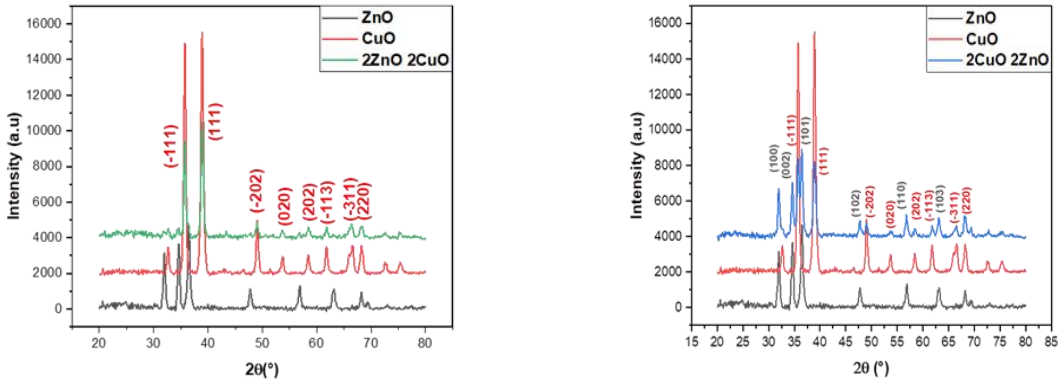

(a) (b)

Figure III.6:X-ray diffraction (XRD) patterns of 2ZnO/2CuO ,2CuO/2ZnO multi thin layers

Crystallite sizes,dislocation density and the micro strain of the deposited films have been calculated using (002) plane for ZnO thin layer and(1 1 1) plane for CuO thin layer as shown on the tableIII.1:

Table III.1 :Crystallite size,Dislocation density and Micro strain of pure ZnO and CuO

	Crystallite size (nm)	Dislocation density(nm^{-2})	Micro strain
Pure ZnO	18.948	2.7×10^{-3}	1.82×10^{-3}
Pure CuO	8,657	0.017	5.26×10^{-2}

III.1. Atomic Force Microscopy (AFM) analysis

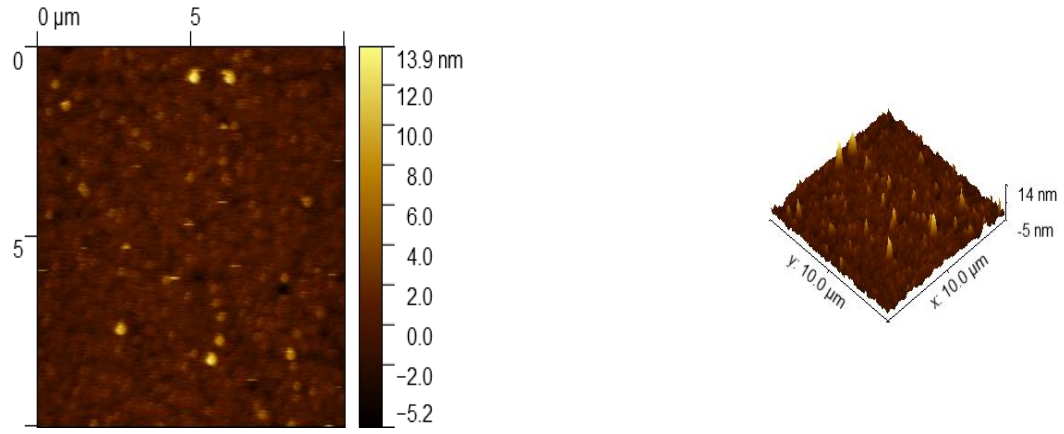

FigureIII.7:10 micron images of pure ZnO thin layer ,2D on the left and 3D on the right

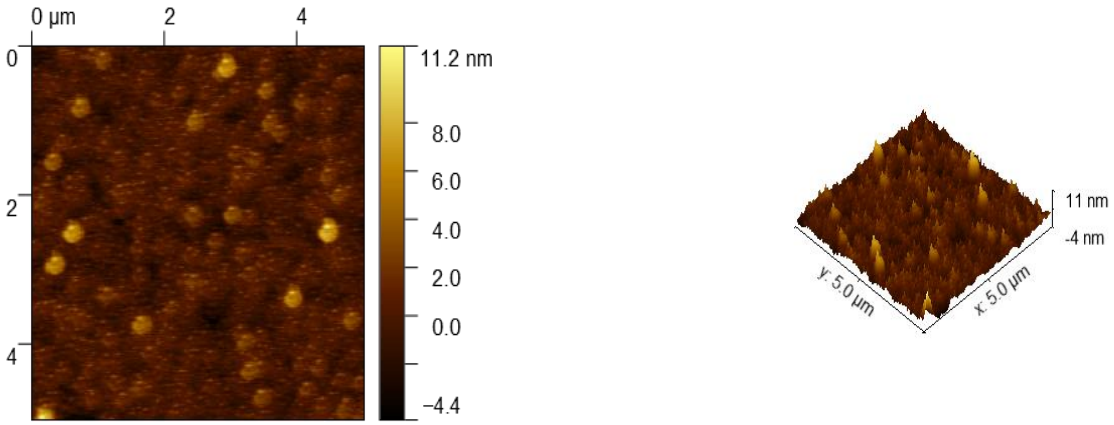

FigureIII.8 :5 micron images of pure ZnO thin layer ,2D on the left and 3D on the right

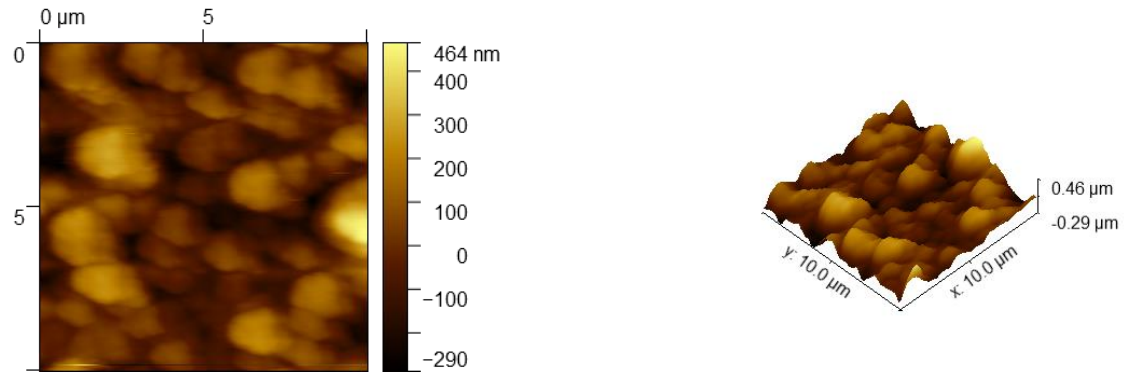

FigureIII.9 :10 micron images of pure CuO thin layer ,2D on the left and 3D on the right

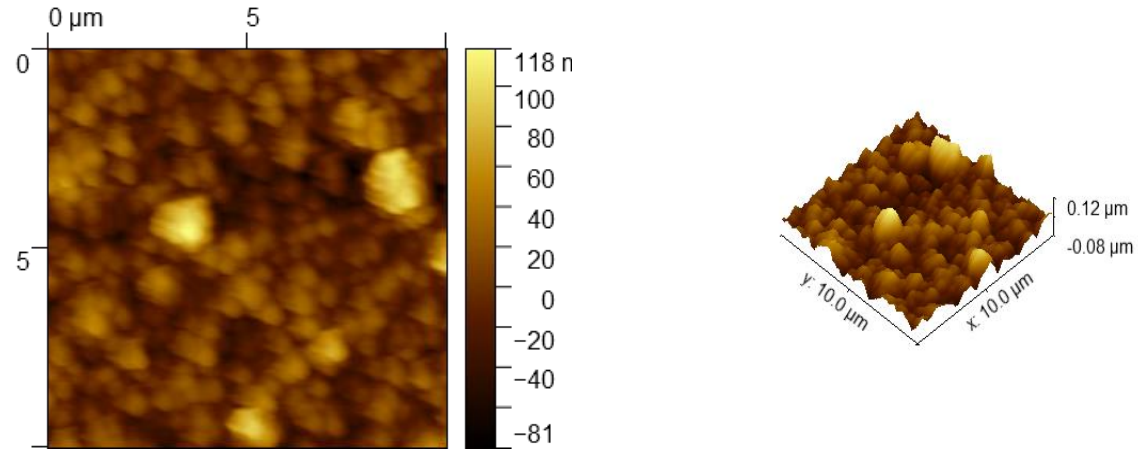

FigureIII.10 :10 micron images of pure ZnO/CuO multi-thin layers ,2D on the left and 3D on the right

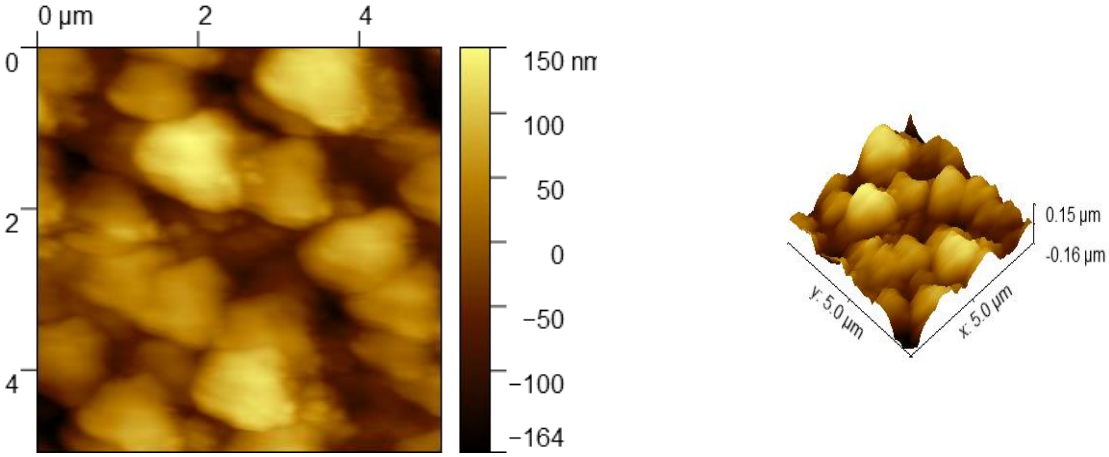

Figure III.11:5 micron images of pure ZnO/CuO multi-thin layers ,2D on the left and 3D on the right

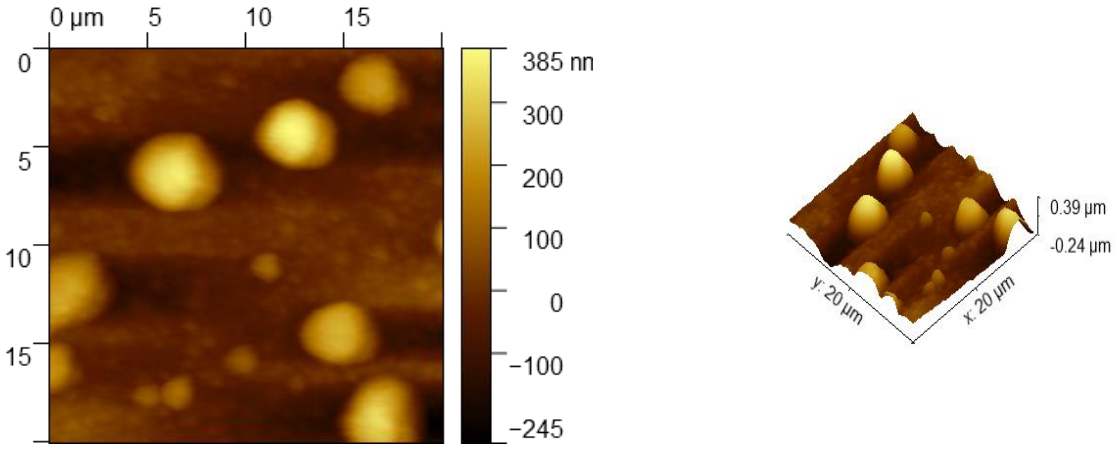

FigureIII.12 :20 micron images of pure 2ZnO/2CuO multi-thin layers ,2D on the left and 3D on the right

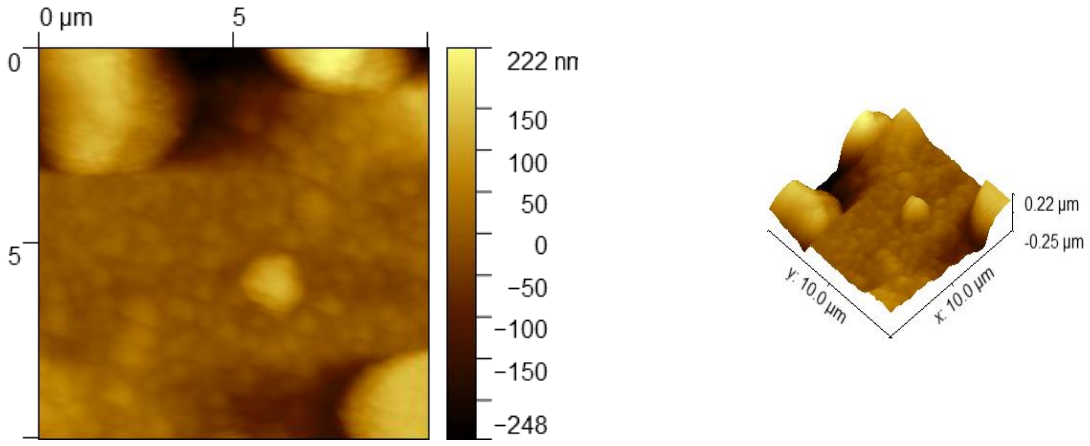

FigureIII.13 :10 micron images of pure 2ZnO/2CuO multi-thin layers ,2D on the left and 3D on the right

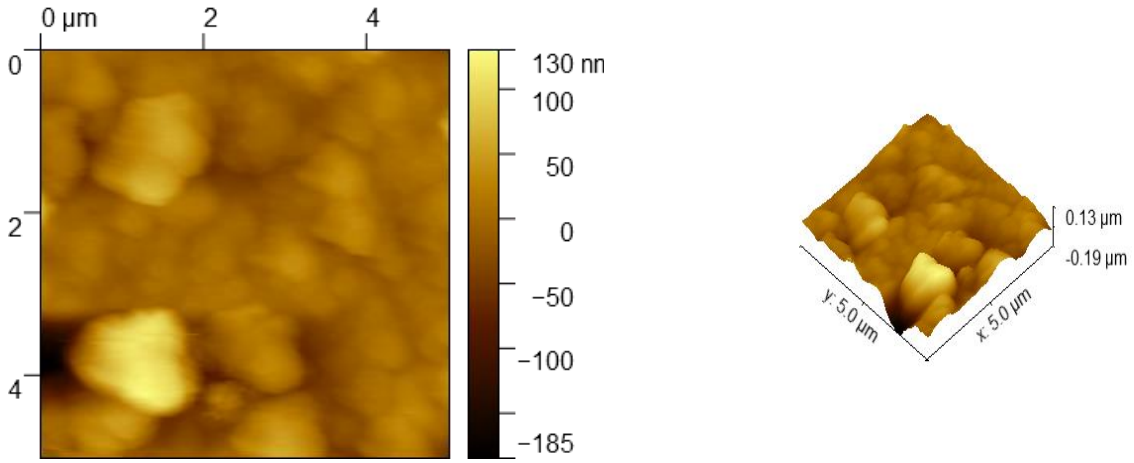

FigureIII.14 :5 micron images of pure 2CuO/2ZnO multi-thin layers ,2D on the left and 3D on the right

These images were taken at various positions on the samples. These images were processed with line by line leveling to normalize the Z range due to the sample stage not being level. In the next part , the data from these images will be analyzed and information about roughness, feature height, and grain analysis will be explored. The 3D images show exaggeration in the Z range in order to display the features on the sample. The color change indicates the height of the sample in the Z range from the dark brown being at zero and the bright yellow being the highest point in the sample[1].

S_q (root mean square roughness), S_{sk} (skewness of sample- degree of distortion from the symmetrical bell curve or the normal distribution), S_{ku} (Kurtosis- measure of whether the data are heavy-tailed or light-tailed relative to a normal distribution) S_p (maximum peak), S_v(valley depth) S_z (maximum height), S_a (arithmetical mean height)[1].

the root mean square roughness (Sq) and the highest peak (Sp)in Z of different samples with deferent micron-scale imagingwere calculated and indicated on the tableIII.2.

Table III.2:Root mean square roughness and Highest peak of deferent samples

Sample		Root mean square roughness (Sq) (nm)	Highest peak (Sp) (nm)
PureZnO	10micron	1.219	13.88
	5 micron	1.327	11.15
Pure CuO	10micron	112.3	463.9
ZnO/CuO	10 micron	22.42	72.1
	5 micron	61.04	203.3
2ZnO/2CuO	20 micron	95.84	385
	10 micron	69.72	221.6
2CuO/2ZnO	5 micron	32.92	129.7

III .3.Fourier Transform Infrared (FTIR) characterization

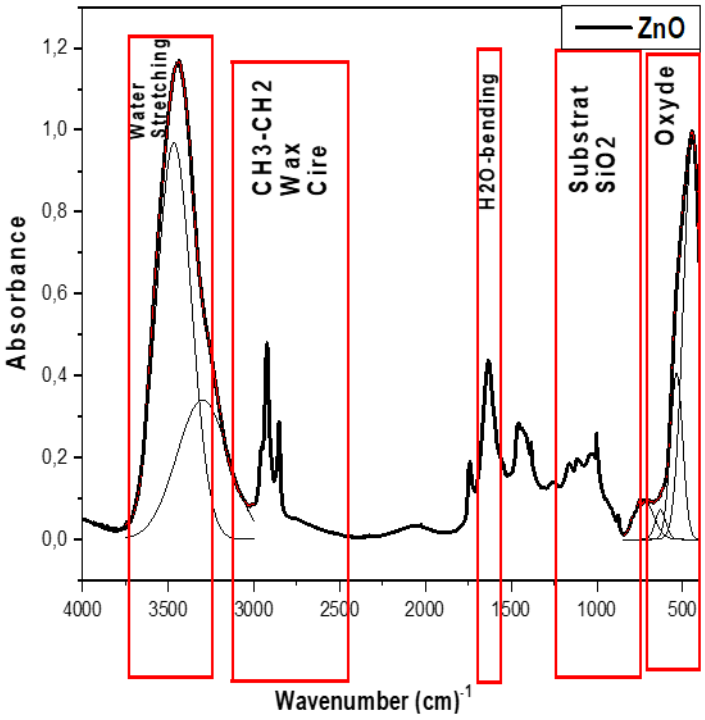

FigureIII .15 : FTIR spectra of ZnO Thin layers

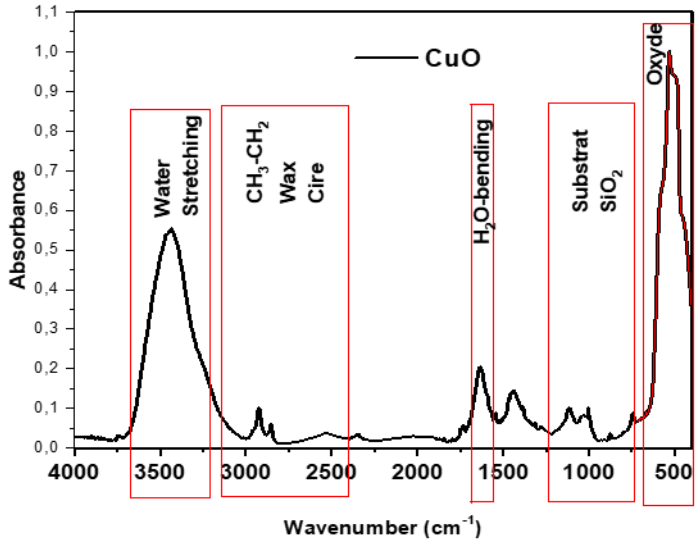

Figure III.16: FTIR spectra of CuO nanoparticles Thin layers

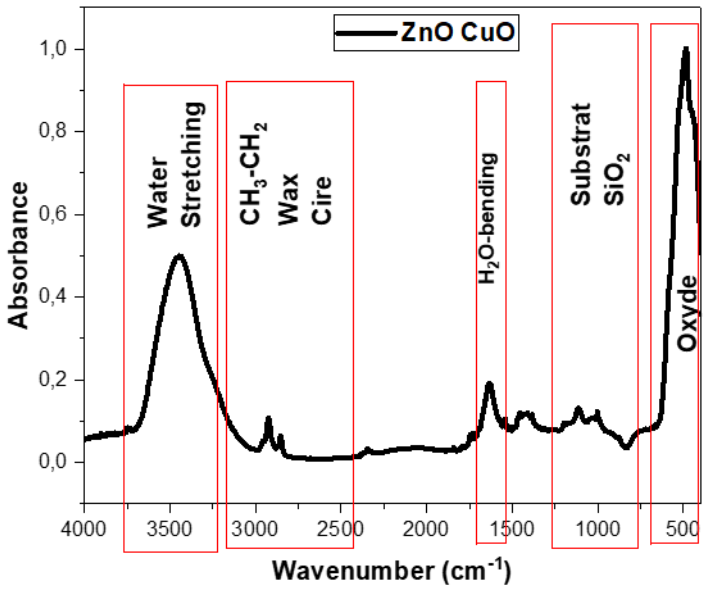

Figure III.17: FTIR spectra of ZnO-CuO nanoparticles Thin layers

Synthesized Zinc Thin layers were subjected to FT-IRanalysis to detect the various characteristic functionalgroup associated with the synthesized thin layers ,figureIII.15.Thepeaks indicate the characteristics functional group presentin the synthesized zinc oxide nanoparticles.It is inferredthat the samples have absorption peaks in the range of 3436 cm^{-1} ,2924 cm^{-1} ,1632 cm^{-1},1004 cm^{-1} ,500 cm^{-1}.The absorption peak at500 cm^{-1}corresponds to metal-oxygen (ZnO stretchingvibrations) vibration mode.The peak at 1004 cm^{-1} isascribed to the stretching vibration of C-N bond of theprimary amine or to the stretching vibration of the C-Obond of the primary alcohol.The peak at1632 $cm^{-1}$is ascribed to the vibration modes of aromaticnitro compounds and alkyl.The peaks at 2924 cm^{-1} and3436 $cm^{-1}$are ascribed to the stretching vibration ofhydroxyl compounds[2].

The FTIR spectrum of synthesized copper oxide Thin layers is presented in Figure III.16. Thepeaks around532 cm^{-1}corresponds to the Cu–O stretching vibration of copperoxide nanoparticles in the monoclinic structure.The absorption band at 1116 cm^{-1} corresponds to the C–O stretching of phenol and alcoholic compoundsThe absorption peaks at 3436 cm^{-1},2924 $cm^{-1}$and 1634 cm^{-1}corresponds to the OH stretching vibration and HOH bending mode of adsorbed watermolecules[3],[4].

In the case of The FTIR spectrum of synthesized Zinc Oxide -Copper Oxide multi-thin layers presented in figureIII.17,peaks indicate the characteristics functional group present only in the Copper Oxide :532 cm^{-1} ,1114 cm^{-1},3446 cm^{-1} .

III .4. UV–visible spectrophotometer analysis

Synthesized thin layers and miltu-thin layers of pure ZnO,pure CuO ,ZnO-CuO,CuO-ZnO,2ZnO-2CuO,2CuO-2ZnO were subjected to UV–visible spectrophotometer analysis which confrms the formation of particles in the initial stage. In the range from 400 to 1000 nm the optical transmittance of pure ZnO was more than 80% , the optical transmittance of pure CuO was 47% at 900 nm ,38% at 1100 nm for ZnO-CuO ,42% at 1100 nm for CuO-ZnO,40% at 1100nm for multi-thin layers 2ZnO-2CuO and 8% at 1100 nm for multi-thin layers 2CuO-2ZnO as showen on figureIII.19.

The optical band gap was estimated by programmsimulationor can be estimated from the first derivative of optical transmittanceand using the equation[5]

$$E_g = \frac{h\vartheta}{\lambda_{max}}$$

FigureIII.20 .

Values are mentionned on the tableIII.3.

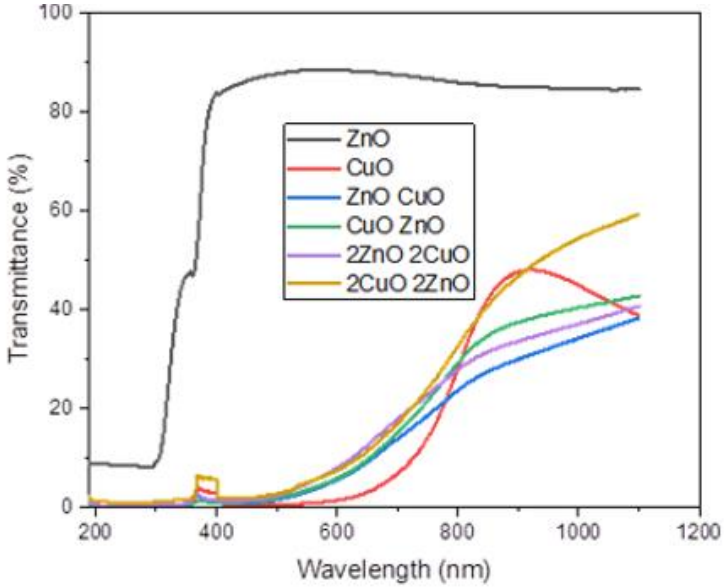

figure III.18:Transmttance spectrum of deferent samples

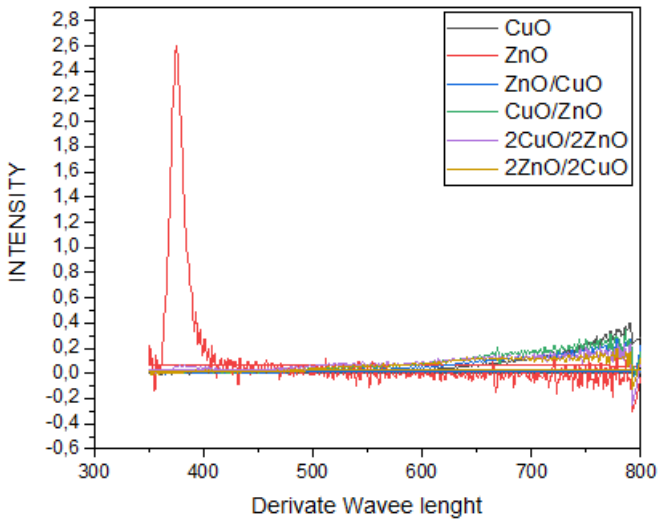

figure III.19:First derivative (dT/dλ) plot of the transmittance spectra.

Table III.3:The optical band gap estimated by program simulation and the first derivative of optical transmittance.

Samples		$E_g$estimated by simulation (Ev)	E_g estimated by using derivative of optical transmittance (Ev)
Pure ZnO		3.42498	3.33
Pure CuO		2.73616	1.58
ZnO-CuO	ZnO	2.50484	3.59
	CuO	2.93098	1.58
CuO-ZnO	CuO	2.02344	1.58
	ZnO	2.32433	3.39
2ZnO-2CuO	ZnO	2.1560	3.13
	CuO	2.0320	1.58
2CuO-2ZnO	C	2.1419	1.56

uO		
Z nO	2.0795	3.21

The results obtained bty the two methods are not close .

The Tauc formula is a widely used empirical equation that relates the absorption coefficient (α) of a material to the photon energy (E) and the band gap energy (Eg). It is commonly employed to estimate the band gap of semiconductors and insulators from optical absorption measurements.

The Tauc formula has some limitations that should be taken into account:

1. Indirect band gap materials: The Tauc formula assumes a direct band gap, where the minimum energy of the conduction band aligns with the maximum energy of the valence band. However, many materials, particularly semiconductors, have an indirect band gap where the minimum energy of the conduction band does not align with the maximum energy of the valence band. In such cases, the Tauc formula may not accurately determine the band gap.

2. Defects and impurities: The Tauc formula assumes perfect crystalline materials without any defects or impurities. However, real-world materials often contain defects or impurities that can introduce energy levels within the band gap. These localized states can significantly affect the absorption spectrum, leading to deviations from the Tauc formula.

3. Quantum confinement effects: The Tauc formula assumes that the absorption edge arises solely from the band gap energy. However, in nanostructured materials like quantum dots or nanocrystals, quantum confinement effects can cause the absorption edge to shift to higher energies due to the discrete energy levels associated with the confinement. The Tauc formula does not account for these effects.

4. Temperature and pressure dependence: The Tauc formula does not consider the temperature and pressure dependence of the band gap. In some materials, the band gap can vary with temperature or under high-pressure conditions. Therefore, the Tauc formula may not accurately estimate the band gap in these situations.

Despite these limitations, the Tauc formula remains a useful tool for estimating the band gap energy of materials based on optical absorption data, especially in cases where the assumptions and conditions are adequately met. However, it is essential to be aware of its limitations and consider alternative methods or more advanced models when dealing with materials that deviate from the assumptions of the Tauc formula.

Copper being multivalent, it forms several oxides; among them, CuO and Cu2O thin films are well known p- type semiconductors; their reported optical band gaps are 1.3 eV - 2.1 eV for CuO and 2.1 eV – 2.6 eV for Cu2O.[6] [7]

References of the chapter

[1] M.McDonough;P. Perov; W. Johnson and S.Radojev , Data Pr Data Processing & Analysis for A ocessing & Analysis for Atomic Force Microscopy (AFM) 2020, Undergraduate Theses and Capstone Projects. 18.

[2] N.Jayarambabu;B.Siva Kumari; K. Venkateswara Raoand Y.T. Prabhu , Germination and Growth Characteristics of Mungbean Seeds (Vigna radiata L.) affected by Synthesized Zinc Oxide Nanoparticles , Department of Botany, Andhra Loyola College, Vijayawada, Andhra Pradesh – India,2014.

[3] A.Varughese et al , Green Synthesis and Characterization of Copper Oxide Nanoparticles Using Psidium guajava Leaf Extract, 2020 IOP Conf. Ser.: Mater. Sci. Eng. 961 012011.

[4] A.Sagadevan Ethiraj and D. Joon Kang, Synthesis and characterization of CuO nanowires by a simple wet chemical method, Research Letters 2012.

[5] S Bouhouche et al 2018 Mater. Effect of Er3+ doping on structural, morphological and photocatalytical properties of ZnO thin films, . Res. Express 5 056407.

[6] Chen, A., Long, H., Li, X., Li, Y., Yang, G., & Lu, P. (2009). Controlled growth and characteristics of single-phase Cu2O and CuO films by pulsed laser deposition. Vacuum, 83(6), 927-930.

[7] Papadimitropoulos, G., Vourdas, N., Vamvakas, V. E., & Davazoglou, D. (2006). Optical and structural properties of copper oxide thin films grown by oxidation of metal layers. Thin Solid Films, 515(4), 2428-2432.

In our study, we successfully confirmed the crystalline structures of ZnO and CuO using XRD analysis and verified the results using the HIGHSCHORE program. We also investigated the differences in the crystalline structures of the ZnO/CuO heterojunction. When CuO was deposited as the top layer, its structure matched that of pure CuO. However, when ZnO was deposited as the top layer, we observed some peaks of ZnO overlapping with the peaks of CuO, likely due to the higher thickness of CuO compared to ZnO.

The estimated crystallite size of pure ZnO, determined from the XRD patterns, was 18.94 nm, while for pure CuO, it was 8,65 nm. The dislocation density and strain in pure CuO samples were higher compared to pure ZnO samples.

Analyzing the micro-scale imaging, we observed different values for the root mean square (Sq) and the highest peak (Sp) among various samples. For pure ZnO samples, the Sq values were 1.229 nm for a 10-micron scale and 1.327 nm for a 5-micron scale. The Sq value of the pure CuO sample was 112.3 nm when measured on a 10-micron scale. For the ZnO/CuO sample, the Sq values were 22.48 nm and 61.04 nm for 10-micron and 5-micron scales, respectively. The 2ZnO/2CuO sample showed Sq values of 95.84 nm and 69.72 nm for 20-micron and 10-micron scales, respectively, while for the 2CuO/2ZnO sample, the Sq value was 32.92 nm when measured on a 5-micron scale. These results indicate that pure ZnO had a smoother surface compared to pure CuO, which had a rougher surface.

Regarding the highest peaks in each sample, we observed the following values: For pure ZnO samples, the highest peak was 13.88 nm for a 10-micron scale and 11.15 nm for a 5-micron scale. The highest peak of the pure CuO sample was 463.9 nm when measured on a 10-micron scale. For the ZnO/CuO sample, the highest peak values were 72.1 nm and 203.3 nm for 10-micron and 5-micron scales, respectively. The 2ZnO/2CuO sample showed highest peak values of 385 nm and 221.6 nm for 20-micron and 10-micron scales, respectively, while for the 2CuO/2ZnO sample, the highest peak was 129.7 nm when measured on a 5-micron scale. These findings support our previous conclusion.

Additionally, we conducted FT-IR analysis on the synthesized Zinc Thin layers to detect characteristic functional groups associated with them. Broad peaks of ZnO were observed, which overlapped with the peaks of CuO.

Furthermore, we performed UV-visible spectrophotometer analysis on the synthesized thin layers of pure ZnO, pure CuO, ZnO-CuO, CuO-ZnO, 2ZnO-2CuO, and 2CuO-2ZnO. The results confirmed the formation of particles in the initial stage. The optical transmittance of

pure ZnO was over 80% in the range from 400 to 1000 nm. For pure CuO, the optical transmittance was 47% at 900 nm, while for ZnO-CuO, it was 38% at 1100 nm. The CuO-ZnO multi-thin layers showed an optical transmittance of 42% at 1100 nm, and the 2ZnO-2CuO multi-thin layers exhibited 40% transmittance at 1100 nm. However, the 2CuO-2ZnO multi-thin layers had only 8% transmittance at 1100 nm.

Based on the transmittance spectrums, the optical band gap values were estimated as follows: pure ZnO had an indirect band gap of 3.33 eV, pure CuO had a band gap of 1.58 eV, ZnO as the bottom layer in ZnO/CuO multi-layers had a band gap of 3.59 eV, and CuO as the top layer in the same multi-layers had a band gap of 1.58 eV. CuO as the bottom layer in CuO/ZnO thin layers had a band gap of 1.58 eV, while ZnO as the top layer in the same multi-layers had a band gap of 3.39 eV. In the 2ZnO/2CuO multi-layers, ZnO as the bottom layer had a band gap of 3.13 eV, and CuO as the top layer had a band gap of 1.58 eV. In the 2CuO/2ZnO multi-layers, CuO as the bottom layer had a band gap of 1.56 eV, and ZnO as the top layer had a band gap of 3.21 eV.

Abstract

This Master's thesis focuses on the synthesis and characterization of thin films of zinc oxide (ZnO), copper oxide (CuO), and ZnO-CuO multilayers. The XRD analysis confirmed the crystalline structures of ZnO and CuO.ZnO deposited as a top layer in the ZnO/CuO heterojunction showed overlapping peaks with CuO, likely due to the higher thickness of CuO.Pure ZnO had a crystallite size of 18.94 nm, while pure CuO had a crystallite size of 8.65 nm. Dislocation density and strain were higher in pure CuO samples compared to pure ZnO samples.The micro-scale imaging revealed that pure ZnO had a smoother surface, while pure CuO had a rougher surface.The optical transmittance of pure ZnO was over 80% in the range from 400 to 1000 nm.The optical transmittance of pure CuO was 47% at 900 nm, and for the ZnO-CuO multi-thin layers, it ranged from 38% to 42% at 1100 nm.The estimated optical band gaps were 3.33 eV for pure ZnO, 1.58 eV for pure CuO, and varied for the multi-layer combinations of ZnO and CuO.

These findings provide comprehensive insights into the structural and optical properties of the synthesized ZnO and CuO thin layers, as well as their multi-layer combinations, highlighting their potential for various applications.

ملخص

تركز أطروحة الماستر هذه على توليف وتوصيف الأغشية الرقيقة من أكسيد الزنك (ZnO) وأكسيد النحاس (CuO) وطبقات متعددة من ZnO-CuO. أكد تحليل XRD الهياكل البلورية لـ ZnO و CuO. أظهر ZnO المودعة كطبقة عليا في التداخل المتغاير ZnO / CuO قمم متداخلة مع CuO ، ويرجع ذلك على الأرجح إلى ارتفاع سمك CuO. كان ZnO النقي بحجم بلوري 18.94 نانومتر ، بينما كان للنحاس النقي حجم بلوري يبلغ 8.65 نانومتر.

كانت كثافة الخلع والضغط أعلى في عينات CuO النقية مقارنة بعينات ZnO النقية. أظهر التصوير على نطاق صغير أن ZnO النقي له سطح أكثر سلاسة ، بينما كان CuO النقي سطحًا أكثر خشونة. تتراوح من 400 إلى 1000 نانومتر ، وكانت النفاذية الضوئية لـ CuO النقي 47 ٪ عند 900 نانومتر ، وبالنسبة للطبقات الرقيقة المتعددة ZnO-CuO ، تراوحت من 38 ٪ إلى 42 ٪ عند 1100 نانومتر ، وكانت فجوات النطاق البصري المقدرة 3.33 eV لـ ZnO النقي ، 1.58 eV لـ CuO النقي ، ومتنوع للتركيبات متعددة الطبقات من ZnO و CuO.

توفر هذه النتائج رؤى شاملة للخصائص الهيكلية والبصرية للطبقات الرقيقة المركبة من ZnO و CuO ، بالإضافة إلى مجموعاتها متعددة الطبقات ، مما يبرز إمكاناتها في التطبيقات المختلفة.